VARIABLE LIFT CONTROL OF A SPACE VEHICLE DURING THE RE-ENTRY INTO MARTIAN ATMOSPHERE

Thesis by
Hiroshi Ohtakay

In Partial Fulfilment of the Requirements
For the Degree of
Doctor of Philosophy

California Institute of Technology
Pasadena, California
1969

(Submitted May 29, 1969)

ACKNOWLEDGEMENT

The author wishes to express sincere appreciation to Professor R. Sridhar for his advice and guidance throughout the course of this investigation. He also wishes to acknowledge Mr. J. Moore, Mr. E. Suggs, Mr. B. Dobrotin and Mr. K. Bouvier for invaluable advice and criticism from an engineering point of view. His gratitude also goes to Dr. W. P. Charette, Dr. G. Ash, and Dr. Y. Sahinkaya, for many useful suggestions and discussions.

During the graduate studies at California Institute of Technology, the author was awarded various Fellowships and Assistantships, for which he is deeply appreciative.

A sincere thank you is extended to Mrs. Paula Samazan for her librarian assistance and to Mrs. Carol Teeter for her magnificent typing.

This work is dedicated to the author's wife, Kikuko, who has been patient, understanding and helpful in putting-husband-through.

ABSTRACT

Re-entry trajectory design problem of a space capsule into the Martian atmosphere is investigated within the context of modern control theory. The optimal control law which minimizes the heat generated on the surface of the capsule is obtained analytically. This in turn allows the capsule to make a successful softlanding on Mars through the partially known atmosphere of the planet. The investigation is also extended to the guidance of the capsule in a stochastic disturbance environment. An attempt is made to simplify the stochastic control law so that the mechanization of the resulting control law is within the grasp of current engineering technology.

TABLE OF CONTENTS

I. INTRODUCTION

In recent years, space technology has made tremedous strides in the exploration of space which has been made possible by launching several satellites into orbit around the earth and interplanetary space vehicles to the moon and Mars. The stringent requirements of space missions such as the control of a particular space vehicle, while minimizing fuel, time, energy or any combination of these, have motivated the use of optimal control theory in the design of appropriate feedback controllers. The optimal control theory has been applied to the solution of aerospace problems such as interplanetary guidance of a space vehicle,[51] automatic aircraft landing,[58] softlanding on the moon[59] and planetary atmospheric re-entry.[2]

Historically, the study of planetary atmospheric re-entry dates back to the early 1930's.[60] Re-entry into earth atmosphere problems have attracted the attention of scientists and engineers in the last two decades.[2,3,4,5,6,7] Optimal control theory has played key roles in the solution[2,3,4] of these problems. The control problems associated with Martian atmospheric re-entry possess the following unique features:

(a) The structure of the atmospheric density model as well as its parameters is not completely known. Quantitatively, the atmospheric density value of Mars is believed[14] to be smaller than that of earth by a factor which ranges from 50 to 200.

(b) The topography of the Martian surface is not known. Hence, the control schemes used for the atmospheric re-entry of the earth[2] do not hold for the Martian atmospheric re-entry.

Currently, there are various methods[1] being considered for injecting a space capsule into an impact trajectory (such as ballistic, gliding, decade orbit, skip and combination of these) of a planetory atmosphere for soft landing. In this investigation two particular trajectory profiles+, namely; atomospheric gliding re-entry with orbits around Mars and direct re-entry, are studied within the context of optimal control theory.

A small number of papers have been published concerning the related topics. The parameter estimation of the Martian atmospheric density model was studied by Cefola[11] using a sensitivity analysis. The minimum terminal speed control problem was investigated by Nieman[12] who has obtained an open loop solution of the problem by trial and error. The Martian atmospheric re-entry of a space capsule, with a constant lift to drag ratio, was studied by Pritchard.[10] No study has ever been reported, to the author's best knowledge, on the gliding type re-entry trajectory design problem within the context of optimal control theory.

Selection of the performance index plays a major role in the correct formulation of a practical optimal control problem. Even though the dynamical equations which describe the behavior of a physical system are properly modeled, an improper choice of the performance index may degrade the optimality of the solution. The minimization of the heat generation of the atmospheric re-entry capsule for an unmanned mission is an important requirement. It is also required that the capsule arrives at its target with a predetermined accuracy even in the

---

+ See Chapter II for details.

presence of stochastic disturbances due to wind and wind gust in the Martian atmosphere.

In Chapter II, two different re-entry trajectory profiles are presented. The analytical expressions for the corresponding trajectories are given.

In Chapter III, a Martian atmospheric re-entry trajectory with minimum heat generation is investigated. The Martian atmospheric density model is represented by an exponential form with known parameters. An approximated control law is obtained in closed form by utilizing the second order theorem of the re-entry dynamics.[5,6,7] It is also shown that the minimum heat generation trajectory is equivalent to the minimum time trajectory. The study is also concerned with a relation between the instantaneous heat generation and the total energy of the capsule.

In Chapter IV, it is shown that the inertial observations can be used as the only available source of the capsule's flight path data. A nonlinear filter is developed to estimate the true atmospheric density parameter as well as the capsule's true flight path. Thus, adaptation of the feedback control system to the partially known atmospheric environment of Mars is shown to be feasible.

In Chapter V, the Martian wind and wind gust models are constructed utilizing Ornstein-Uhlenbeck processes.[50] A stochastic optimal control problem is formulated to investigate the minimum energy thrust program to cope with the stochastic disturbances. Feasibility of the formulation is demonstrated by using Monte Carlo simulations.[57] A suboptimal control law is obtained in order to facilitate a feasible

implementation of the resulting control law.

II. TRAJECTORY PROFILES

2.1 Introduction

During interplanetary flight, the spacecraft consists[18] of the bus and the capsule. The atmospheric impact trajectory is initiated by separating the capsule from the bus, and placing the capsule into an atmospheric re-entry trajectory. There are two ways of accomplishing this task: One is the orbit re-entry trajectory[18] and the other is the direct re-entry trajectory. Two dimensional descriptions of these trajectories are illustrated in Figure 1. Attention is focused on the orbit re-entry scheme throughout this investigation: The direct re-entry case is also studied for the sake of comparison.

Re-entry of the space capsule into the Martian atmosphere can be categorized into three phases;[15] the approach phase, the atmospheric re-entry phase and the soft landing phase.

The approach phase, in both direct re-entry and orbit re-entry, starts when the space vehicle separates into two parts, the atmospheric re-entry capsule and the bus. The main purpose of this investigation is to study the control of the atmospheric re-entry capsule. The terminal point of the approach phase is defined as the point when the capsule touches the fictitious atmospheric boundary.+

The atmospheric re-entry phase is assumed to be initiated at an altitude of about 30.0×10^4 ft. At this height, the most plausible Martian atmospheric density model,[14,18] VM-4, assumes a value of 10^{-11} slug/ft^3. The destination point of this phase is defined arbi-

---

+ See Section 3.2.1 for definition.

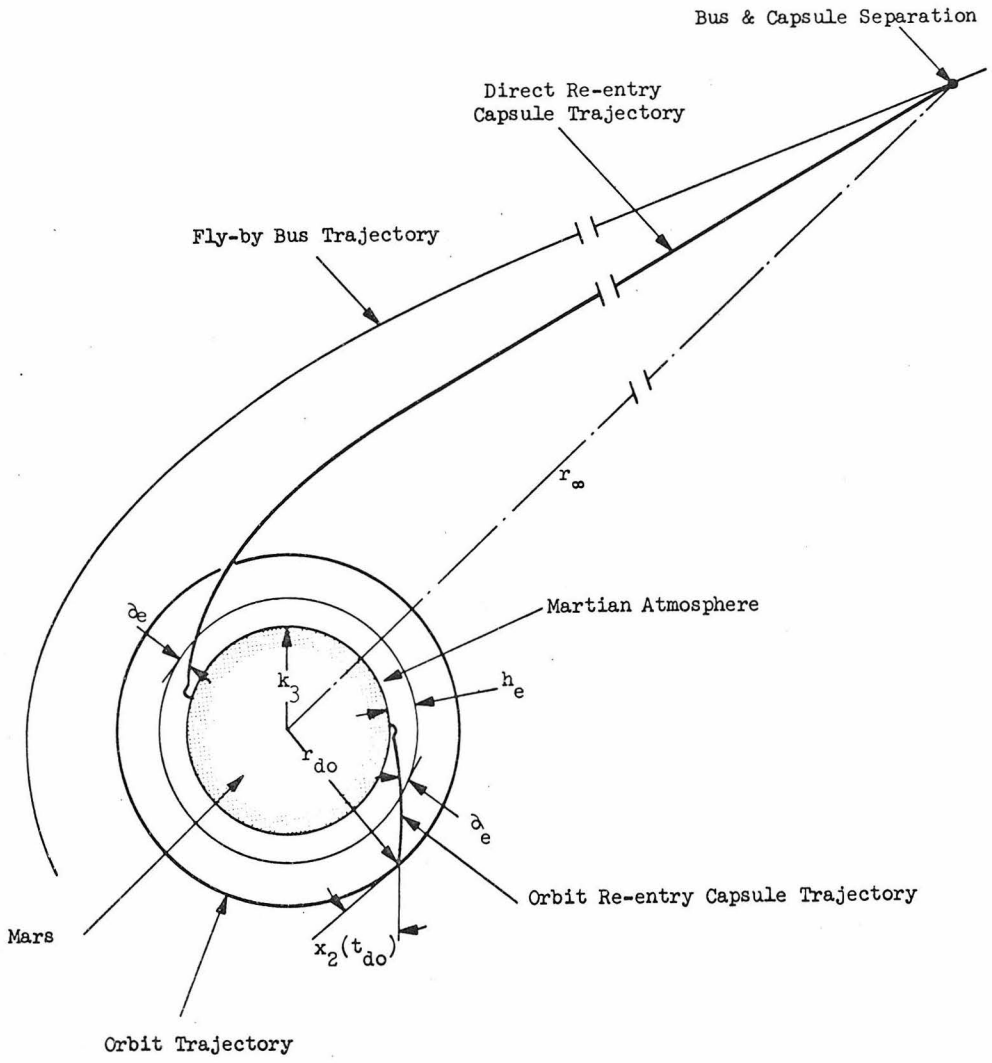

Figure 1. Direct and orbit re-entry trajectories of the capsule.

trarily as the point at which the capsule arrives at an altitude of 15.0×10^3 ft. In order to initiate a descent of the capsule for soft landing, the speed of the capsule must be somewhat less than 1.00×10^3 ft/sec.[13]

The last phase which is the soft landing phase starts at an altitude of 15.0×10^3 ft. Either parachute[9] or retro rocket[8,13] is assumed to be used for the braking mechanism. During the flight of the capsule in this phase, radar altitude and doppler velocity measurements will be made.[13] By using these measurements, it becomes possible to perform a finer control of the capsule's maneuver in order to accomplish a soft and vertical landing of the capsule. The soft landing is accomplished properly if the capsule's vertical velocity is less than 25 ft/sec, its final horizontal velocity is less than 5 ft/sec and its attitude is within 10 degrees from the local vertical.

2.2 Assumptions

The following assumptions are made during the course of this investigation:

(a) Motions of the capsule and the bus are restircted in a plane.

(b) Mars is a non rotating perfect sphere and its mass is uniformly distributed around the centre of the planet.

(c) The landing site of the re-entry capsule and the time of the mission are arbitrary.

(d) Martian atmosphere is homogeneous and stationary with its density being given by exponential models (see Section 3.2.1 for details).

Among these assumptions, restriction (d) will be relaxed in the dis-

cussion section of Chapter V.

2.3 Coordinate System and Dynamics

The origin of the Cartesian coordinate system is located at the centre of gravity of the capsule. One of the axes lies in the direction of the velocity vector.

It is assumed that the only gravitational force acting on the dynamical system is originated at the centre of Mars. The planar motion of the dynamical system with respect to the centre of Mars is characterized by[+]:

$$\frac{dx_1}{dt} = \frac{k_{13}}{(x_3 + k_3)^2} \cdot \sin x_2 - T_n \quad . \tag{2.1}$$

$$x_1 \frac{dx_2}{dt} = - x_1^2 \frac{\cos x_2}{x_3 + k_3} + k_{13} \frac{\cos x_2}{(x_3 + k_3)^2} - T_t \tag{2.2}$$

$$\frac{dx_3}{dt} = - x_1 \sin x_2 \quad . \tag{2.3}$$

The external torques, T's, are given, in the approach phase, by:

$$T_t = 0 \qquad T_n = 0 \tag{2.4}$$

+ All symbols are defined in Nomenclature in Appendix A.

and, in the atmospheric re-entry phase, by:

$$T_t = \frac{1}{m}(L + \ell)$$
$$T_n = \frac{1}{m}(D + d) \qquad (2.5)$$

where

$$L \triangleq \frac{A_o C_L}{2} \rho(x_3)\, x_1^2 \qquad (2.6)$$

= (gasdynamic lift)

$$D \triangleq \frac{A_o C_D}{2} \rho(x_3)\, x_1^2 \qquad (2.7)$$

= (gasdynamic drag)

d, ℓ = stochastic disturbances

2.4 Orbit Re-entry

The orbit re-entry can be characterized as follows: The space vehicle consisting of the capsule and the bus is put into an orbit trajectory around Mars. This parking orbit may be either circular or elliptical. The orbit determination is completed[20,21] in about two days after the insertion of the vehicle into orbit. This in turn allows the identification of the position and the velocity of the space vehicle quite accurately. Furthermore, by utilizing accelerometer and gyros on board, it is also possible[16] to observe the velocity, the flight path angle and the altitude inertially during the atmospheric re-entry

phase. The de-orbit maneuver of the capsule takes place under the control of a pre-entry system and according to the following sequence:[18] The capsule is separated from the bus. Then, the capsule is placed into the approach phase trajectory, while the bus stays on orbit. The nominal velocity after the separation is assumed to be

$$x_1(t_{do}) = 15.6 \times 10^3 \quad \text{ft/sec} \tag{2.8.1}$$

at an altitude of

$$x_3(t_{do}) = 80.0 \times 10^4 \quad \text{ft.} \tag{2.8.2}$$

The nominal trajectory of the capsule is given by the solution of Eqs. (2.1) through (2.4). It is a hyperbolic trajectory[19] which satisfies the relation such as:

$$x_1^2(t) = x_1^2(t_{do}) + 2k_1\{x_3(t_{do}) - x_3(t)\} \tag{2.9.1}$$

and

$$x_1(t)\ \{x_3(t) + k_3\} \cos x_2(t) = \text{constant} \tag{2.9.2}$$

Therefore, the nominal velocity, $x_1(t_e)$, when the capsule hits the atmospheric boundary, $x_3(t_e)$, is given by:

$$x_1(t_e) \triangleq v_e = 16.0 \times 10^3 \quad \text{ft/sec}$$
$$x_3(t_e) \triangleq h_e = 30.0 \times 10^4 \quad \text{ft.} \tag{2.10}$$

Eq. (2.9.2) and those nominal values indicate that the flight path angle, $x_2(t_{do})$, after separation must be within the re-entry corridor such as:

$$\gamma_s < x_2(t_{do}) < \gamma_c \tag{2.11}$$

where

$\gamma_s \triangleq$ skip out angle[+]

$\gamma_c \triangleq$ critical angle[++]

2.5 Direct Re-entry

The approach phase of the direct re-entry scheme is also initiated by separation of the capsule from the bus. However, the separation takes place at a relatively large distance[10] from Mars. This prevents the fly-by bus from impacting on the planet even though

---

+ The shallowest possible atmospheric re-entry angle at which the capsule can be captured by the atmosphere.

++ The largest possible atmospheric re-entry angle at which the flight path angle exceeds the maximum value of 90 degrees at least once before the capsule arrives at the target.

separation velocities are very small.[10] Hence, separation is assumed to take place at a distance of

$$x_3(t_\infty) = 300\ k_3 \quad \text{ft} \tag{2.12.1}$$

away from the surface of Mars. The nominal velocity of the capsule after separation is assumed to be

$$x_1(t_\infty) = 20.2 \times 10^3 \quad \text{ft/sec.} \tag{2.12.2}$$

Then, the capsule flies along the hyperbolic trajectory+ given by:

$$x_1^2(t) = x_1^2(t_\infty) - \frac{2k_{13}}{x_3(t_\infty) + k_3} + \frac{2k_{13}}{x_3(t_\infty) + k_3} \tag{2.13}$$

$$x_1(t)\ \{x_3(t) + k_3\} \cos x_2(t) = \text{constant.}$$

The nominal velocity, $x_1(t_e)$, of the capsule at the boundary, $x_3(t_e)$, of the atmopshere is given by:

$$\begin{aligned} x_1(t_e) &\triangleq v_e = 26.0 \times 10^3 \quad \text{ft/sec.} \\ x_3(t_e) &\triangleq h_e = 30.0 \times 10^4 \quad \text{ft.} \end{aligned} \tag{2.14}$$

In order for the re-entry angle to be within the allowed re-entry corridor, i. e. Eq. (2.11), the flight path angle after separation must be

$$\cos^{-1}\{\delta \cos \gamma_s\} < x_2(t_\infty) < \cos^{-1}\{\delta \cos \gamma_c\} \tag{2.15}$$

+ The trajectory of the bus is also determined to be hyperbolic.

where

$$\delta = 4.28 \times 10^{-3} \ .$$

In order to attain this accuracy, a celestial observation for trajectory determination as well as a finer approach guidance[51] control may be required. It has been merely assumed that such requirement is accomplished.

III. DETERMINISTIC OPTIMUM CONTROL PROBLEM

3.1 Introduction

In this chapter, the formulation and the solution of the optimal control problem is presented for the deterministic case. By deterministic case it is meant that all the parameters of the Martian atmosphere as well as its structure are known. It is also implied that noise free measurements of all state variables are available at each instant of time. However, in the real situation the problem is much more complicated, that is; the Martian atmospheric structure is partially known;[14] only the range of atmospheric density values are specified;[14] the observable state variables are noise corrupted;[16] the dynamical motion of the capsule is subject to stochastic disturbances. In order to circumvent these difficulties, suitable assumptions have been made in order to obtain a closed loop solution of this optimization problem. The complete mathematical descriptions of the capsule's flight dynamics are given by Eqs. (2.1) through (2.3), in which the external torques, T_t and T_n, are due to gasdynamic lift and drag, respectively. A suitable control force is defined to be the ratio of the lift to drag. For obvious practical reasons, the absolute value of this control is bounded.[61] The controllability of this system is verified through several computer simulations for a set of plausible initial conditions. The approximate solution of the control problem has the same order of accuracy as that given by the second order theorem of a re-entry mechanism.[5,6,7]

The optimal trajectory is designed in such a way that the heat generation around the capsule is minimized during the atmospheric

re-entry phase. Bellman's dynamic programming[47] technique and Pontryagin's maximum principle[29] are the main tools which are utilized in the solution of this control problem. Atmospheric density models with constant temperature are assumed in the stratosphere: In the troposphere use is made of atmospheric density models of exponential type which are the approximations of the linear temperature models[14,17,18] suggested by NASA.

3.2 Formulation of the Problem

3.2.1 Atmospheric Density Models[14,17,18]

A typical Martian atmospheric model consists of two layers, the troposphere and the stratosphere. In the troposphere, which stretches from zero altitude to the tropopause height denoted by k_{12}, it is assumed that the atmospheric temperature decreases linearly with altitude in NASA - JPL models[14,18] of Martian atmosphere. Thus, the barometric equation given by:

$$\frac{dP}{dx_3} = - k_1 \rho(x_3) \tag{3.1}$$

in a constant gravitational field yields[33] an atmospheric density model such as:

$$\rho(x_3) = \rho_{ot}\left(\frac{T_o + \Gamma x_3}{T_o}\right)^{-\left(1 + \frac{k_1 M}{\Gamma R}\right)} \tag{3.2}$$

where an ideal gas law is assumed. On the other hand, the stratosphere, which is adjacent to the troposphere, is assumed to be at a constant

temperature. Therefore, Eq. (3.1) yields an atmospheric density model in the stratosphere such as:

$$\rho(x_3) = \rho_{os} e^{-\beta_s x_3} \tag{3.3}$$

It is quite convenient, however, for the purpose of parameter estimation to use similar expressions in both stratosphere and troposphere models. Thus, Eq. (3.2) is approximated by an exponential function such as:

$$\rho(x_3) = \rho_{ot} e^{-\beta_t x_3} \tag{3.4}$$

Two extreme models,[14,18,22] VM-8 and VM-10, and an average model, VM-4, of the Martian atmospheric density are illustrated in Figure 2. The corresponding parameter values are tabulated in Table 1.

A fictitious atmospheric boundary is set around Mars. It is assumed to be at the height of

$$h_e = 30.0 \times 10^4 \text{ ft}$$

above the surface of Mars. This is the altitude at which the most realistic atmospheric density model, VM-4, takes the value of about 10^{-11} slug/ft^3, and the gasdynamical effect acting on the capsule becomes insignificant.

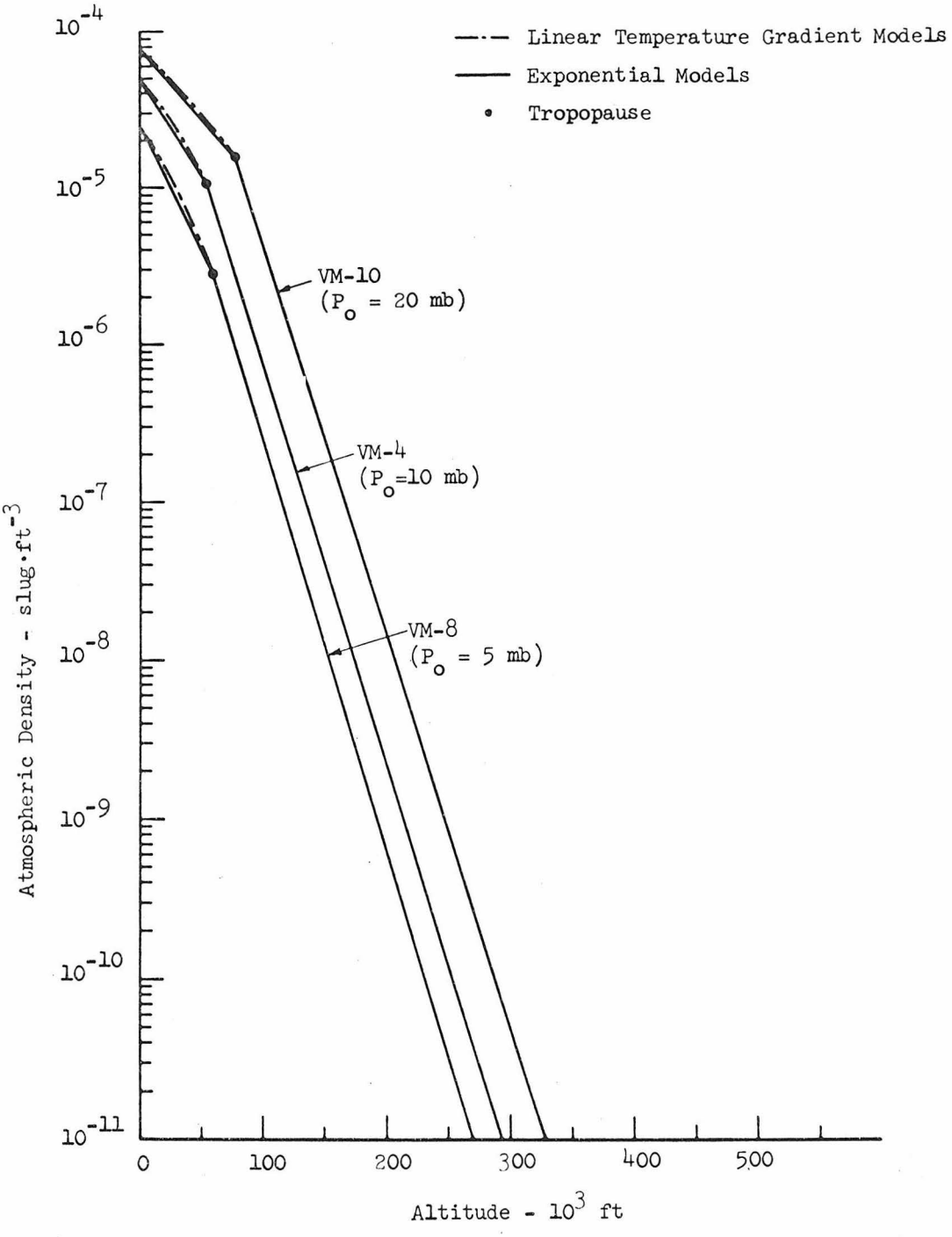

Figure 2. Martian atmospheric density models: VM-4, VM-8 and VM-10.

	Symbol	Dimension	VM - 4	VM - 8	VM - 10
Surface Pressure	P_o	mb	10.0	5.00	20.0
Surface Density (Troposphere)	ρ_{ot}	slugs/ft^3	4.98×10^{-5}	2.56×10^{-5}	7.44×10^{-5}
Surface Density (Stratrosphere)	ρ_{os}	slugs/ft^3	2.76×10^{-4}	1.61×10^{-4}	4.20×10^{-4}
Surface Temperature	T_o	^oK	200.	200.	200.
Acceleration of Gravity at Surface	g	ft/sec^2	12.3	12.3	12.3
Molecular Weight	M	mol^{-1}	42.7	44.0	31.9
Adiabatic Lapse Rate	Γ	^oK/Km	-5.85	-5.39	-4.33
Tropopause Altitude	h_T	ft	56.1×10^3	61.0×10^3	75.8×10^3
Inverse Scale Height (Troposphere)	β_t	ft^{-1}	2.84×10^{-5}	3.05×10^{-5}	2.13×10^{-5}
Inverse Scale Height (Stratosphere)	β_s	ft^{-1}	5.89×10^{-5}	6.07×10^{-5}	4.41×10^{-5}
Surface Wind Speed	$\bar{\omega}$	ft/sec	156.0	220.0	110.0
Maximum Wind Speed$^+$	w_1	ft/sec	310.0	450.0	225.0
Maximum Gust Speed	w_2	ft/sec	150.0	200.0	100.0

Table 1. Martian Atmospheric Density Models

$^+$ In altitude between 1000 ft and $90. \times 10^3$ ft.

3.2.2 Definition of Control Force

It is the purpose of this investigation to reduce the speed of the capsule by utilizing gasdynamic braking effect while controlling the aerodynamic lift. The control force must be such that it can transfer the state of the system, i.e. (x_1, x_2, x_3), from the initial set, i.e. (v_e, α_e, h_e), to the terminal set, i.e. (v_f, α_f, h_f). It is highly desired that the control force be independent of the atmospheric density. Therefore, the gasdynamic lift to drag ratio such as:

$$L/D = C_L/C_D \tag{3.5}$$

is selected to be the available control force. The absolute value of this quantity could be bounded from above because of the fixed aerodynamic structure of the capsule.[61] This quantity could be changed continuously within certain bounds with sophisticated mechanization. Note however that it is desirable to have a simple control scheme rather than a sophisticated one. In this investigation the control force is restricted only to the following possible values such as:

$$u \triangleq L/D \in U \tag{3.6}$$

where

$$U \triangleq \{ + u_o, - u_o \}$$

= a set of admissible control.

Methods of mechanizing this type of control forces are given in the following discussion: One form of implementation is achieved

by rolling the capsule around its stability axis so that only the direction of the lift is changed without affecting either magnitude or orientation of the drag. Other form of implementation is achieved[5] by installing a flap (or flaps) to the capsule. Movement of the flap produces the desired control forces. Figure 3 illustrates the above mechanizations.

3.2.3 Terminal Speed

It is desired that the speed of the capsule be as small as possible at the end of the atmospheric re-entry phase. It is also required that the terminal speed, denoted by v_f, should be controlled to be invariant for different atmospheric density models. This is due to the fact that the motion of the capsule in the soft landing phase is dominated[8] by the gravitational force and the braking effect produced by a retro rocket or parachute. The lowest attainable speed in the atmospheric re-entry phase is defined as the one at which the atmospheric re-entry trajectory terminates, and no lower speed is taken throughout the atmospheric re-entry phase. Then, it is apparent that this minimum speed, denoted by v_f, is attained when the deceleration becomes zero, i.e.

$$\frac{dx_1}{dt} = 0 \quad .$$

This condition in Eq. (3-12) yields:

$$x_1(t_f) \triangleq v_f = \left\{\frac{2k_1k_2}{\rho(h_f)} \sin \alpha_f\right\}^{\frac{1}{2}} \quad . \tag{3.7}$$

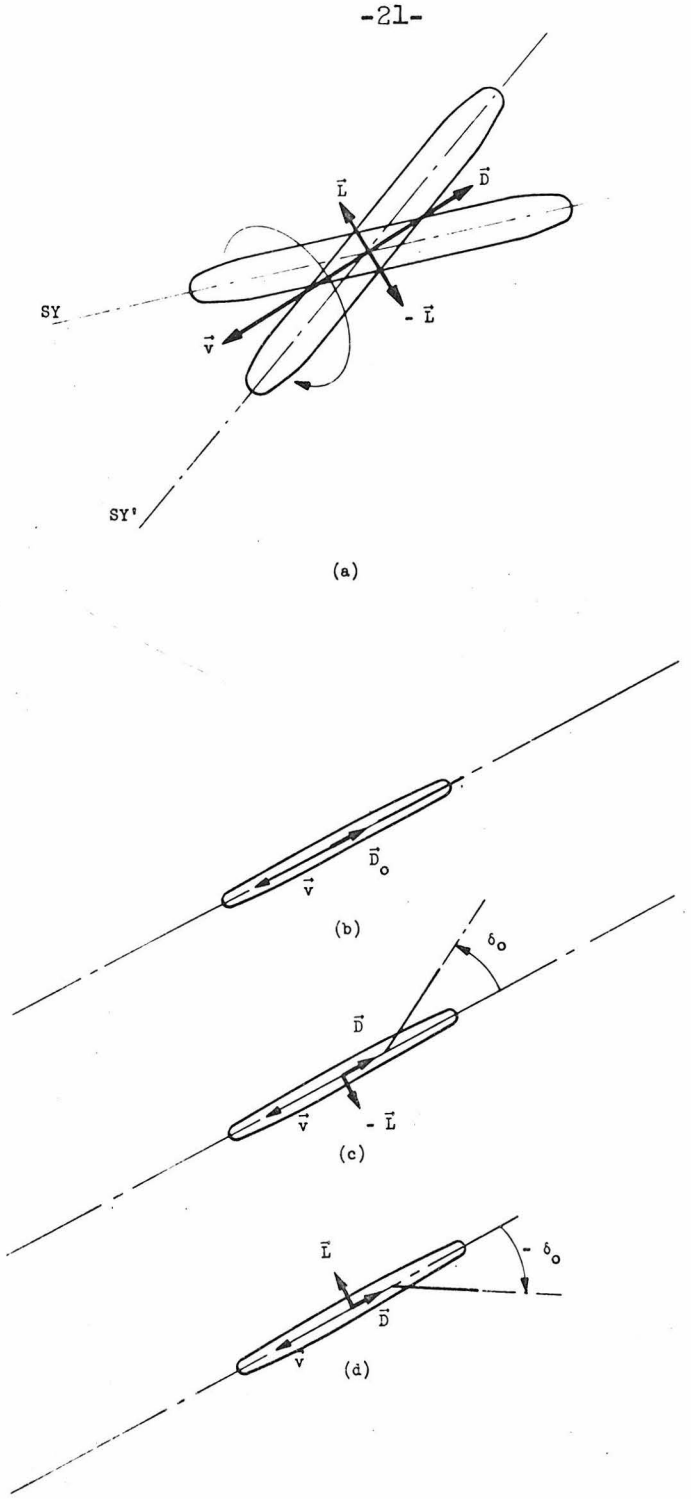

Figure 3. Mechanization of variable lift to drag ratio control: (a) by rotation of the capsule; (b), (c), (d) by a flap.

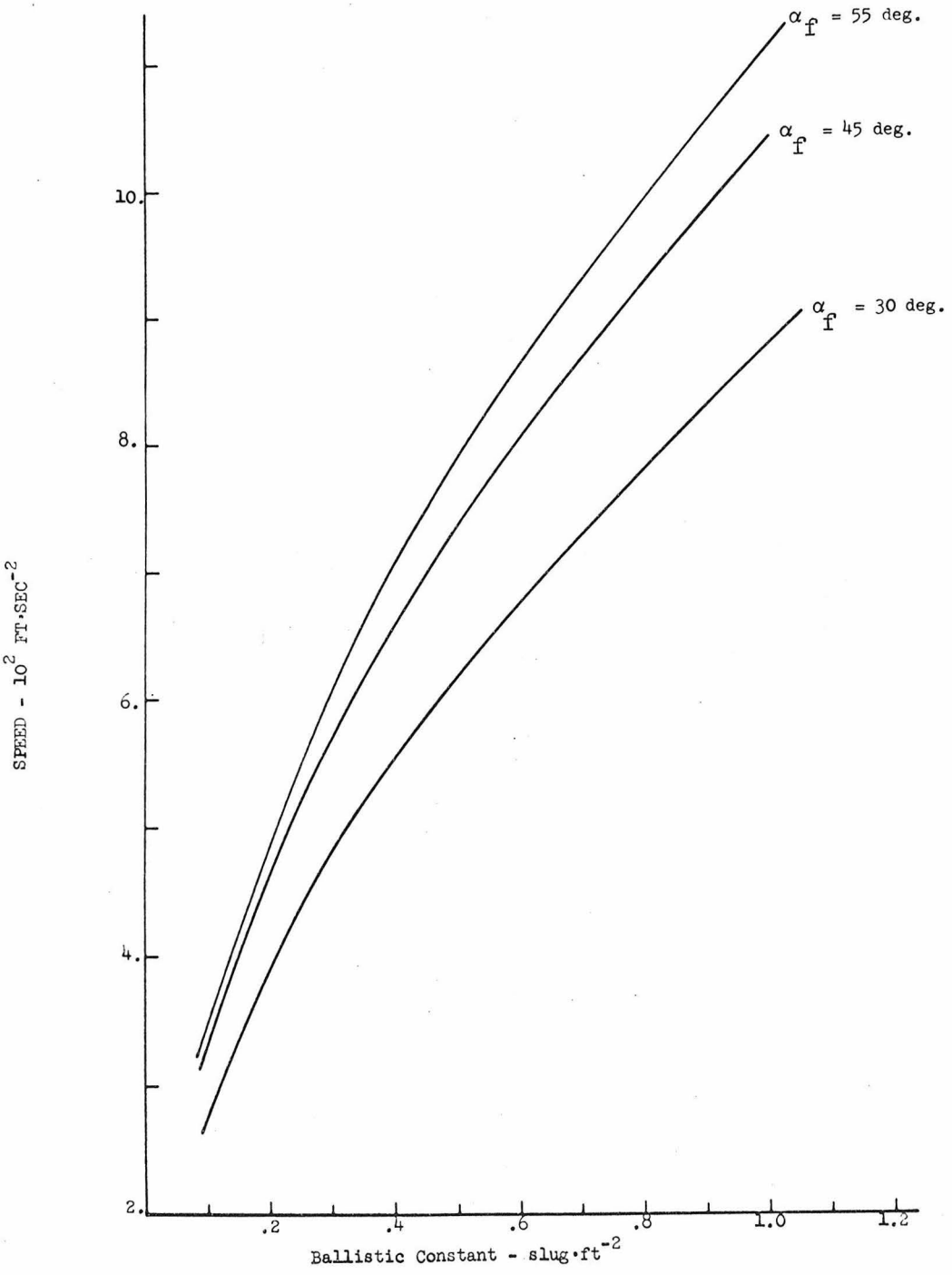

Figure 4. Terminal speed of re-entry capsule versus ballistic constant.

In order to assure the invariance of the terminal speed among different atmospheric density models, the worst case v_f is selected. That is, in Eq. (3.7), ρ is given by:

$$\rho(h_f) = \rho_8(h_f) \quad .$$

3.2.4 Presentation of the Problem

It is assumed that the heat generation at any part of the capsule is proportional[25] to that of the stagnation point. Hence, it is intended to minimize the total heat transfer, denoted by Q_T, due to[+] convection. The quantity such as[++]:

$$Q_T \triangleq \int_{t_e}^{t_f} k_9 \, x_1^3 \, \rho^{\frac{1}{2}}(x_3) \, dt \quad \text{BTU/FT}^2, \tag{3.8}$$

where

$$k_9 = 20.4 \times 10^{-9} \, R_n^{-\frac{1}{2}} \, , \tag{3.9}$$

plays the role of the performance index in the optimal control problem presented below: The state of the system is desired to be transferred

---

[+] Radiative heat transfer is neglected since its contribution[10,23] is much less than 20 per cent of the total heat transfer.

[++] For definition of symbols, see Nomenclature of Appendix A.

from[+]

$$x_1(t_e) = 16.0 \times 10^3 \quad \text{ft/sec}$$

$$x_2(t_e) = \text{unspecified} \tag{3.10}$$

$$x_3(t_e) = 30.0 \times 10^4 \quad \text{ft}$$

to the target

$$x_1(t_f) = v_f \quad \text{ft/sec}$$

$$x_2(t_f) = \text{unspecified} \tag{3.11}$$

$$x_3(t_f) = 15.0 \times 10^3 \quad \text{ft}$$

in such a way that the performance index (3.8) is minimized, with respect to the control force u, under the constraint of the system of differential equations such as:

$$\frac{dx_1}{dt} = k_1 \sin x_2 - \frac{\rho(x_3)}{2k_2} x_1^2 \tag{3.12}$$

$$\frac{dx_2}{dt} = \left(\frac{k_1}{x_1} - \frac{x_1}{k_3}\right) \cos x_2 - u \frac{\rho(x_3)}{2k_2} x_1 \tag{3.13}$$

$$\frac{dx_3}{dt} = - x_1 \sin x_2 \tag{3.14}$$

[+] For direct re-entry, the initial condition for x_1 is given by

$$x_1(t_e) = 26.0 \times 10^3 \quad \text{ft/sec.}$$

where

$$\rho(x_3) \triangleq \begin{cases} k_6 \exp[-k_7 x_3] \text{ for } x_3 < k_{12} \\ k_4 \exp[-k_5 x_3] \text{ for } x_3 \geq k_{12} \end{cases} . \tag{3.15}$$

The time period, $t_f - t_e$, during which the control action takes place, is unspecified. This problem has one more constraint. That is, one of the state variables has an inequality constraint given by:

$$s \triangleq k_8 - x_3 \leq 0. \tag{3.16}$$

where k_8 is the lowest attainable altitude of the capsule before it arrives at the target. This condition is necessary in order to prevent the capsule from crashing into the ground.

3.3 Solution of the Problem

3.3.1 Formal Solution

The penalty function method[32] is used to solve the problem with a state variable inequality constraint, within the framework of optimal control theory. That is, in order to avoid the inequality constraint given by Eq. (3.16), a penalty function, denoted by $x_4(t)$, is defined as:

$$x_4(t_f) = \int_{t_e}^{t_f} (k_8 - x_3)^2 \, Q(s)dt \quad , \tag{3.17}$$

where

$$Q(s) = \begin{cases} 0 & \text{if } s \leq o \\ K & \text{if } s > o \end{cases}$$

$K \triangleq$ a positive constant.

The penalty function is also written in a differential form such as:

$$\frac{dx_4}{dt} = (k_8 - x_3)^2 \, Q(s) \; . \tag{3.18}$$

The boundary conditions for this state variable are

$$\left.\begin{aligned} x_4(t_e) &= 0 \\ x_4(t_f) &= 0 \end{aligned}\right\} \tag{3.19}$$

for the optimal trajectory. Adjoining Eq. (3.17) to the original system of Eqs. (3.12) through (3.14), and letting

$$\lambda \triangleq \text{col } (\lambda_1, \lambda_2, \lambda_3, \lambda_4)$$

be the corresponding vector valued Lagrange multiplier, then Potryagin's maximum principle[29] converts the original problem into a nonlinear two point boundary value problem (TPBVP). That is, if

$$\hat{x} \triangleq (\text{the optimal trajectory of } x),$$

then each element of $\hat{x}$ as well as of λ is given by the solution of the following equations:

$$\frac{d\hat{x}_1}{dt} = k_1 \sin \hat{x}_2 - \frac{\rho(\hat{x}_3)}{2k_2} \hat{x}_1^2 \tag{3.20}$$

$$\frac{d\hat{x}_2}{dt} = \left(\frac{k_1}{\hat{x}_1} - \frac{\hat{x}_1}{k_3}\right) \cos \hat{x}_2 - u_o \frac{\rho(\hat{x}_3)}{2k_2} \hat{x}_1 \operatorname{sgn}(\lambda_2) \tag{3.21}$$

$$\frac{d\hat{x}_3}{dt} = - \hat{x}_1 \sin \hat{x}_2 \tag{3.22}$$

$$\frac{d\hat{x}_4}{dt} = (k_8 - \hat{x}_3)^2 \, Q(S) \tag{3.23}$$

$$\frac{d\lambda_1}{dt} = - 3k_9 \rho^{1/2}(\hat{x}_3)\hat{x}_1^2 + \lambda_1\{\frac{\rho(\hat{x}_3)}{k_2} \hat{x}_1\} + \lambda_2\{(\frac{k_1}{\hat{x}_1^2} + \frac{1}{k_3}) \cos \hat{x}_2 + u_o \frac{\rho(\hat{x}_3)}{2k_2} \operatorname{sgn}(\lambda_2)\}$$

$$+ \lambda_3 \sin \hat{x}_2 \tag{3.24}$$

$$\frac{d\lambda_2}{dt} = - \lambda_1\{k_1 \cos \hat{x}_2\} + \lambda_2 \{(\frac{k_1}{\hat{x}_1} - \frac{\hat{x}_1}{k_3}) \sin \hat{x}_2\} + \lambda_3\{\hat{x}_1 \cos \hat{x}_2\} \tag{3.25}$$

$$\frac{d\lambda_3}{dt} = \frac{k_9 k_5}{2} \rho^{1/2}(\hat{x}_3)\hat{x}_1^3 - \lambda_1\{\frac{k_5 \rho(\hat{x}_3)}{2k_2} \hat{x}_1^2\} - \lambda_2\{\frac{k_5}{2k_2} \rho(\hat{x}_3)\hat{x}_1 \operatorname{sgn}(\lambda_2)\}$$

$$+ 2\lambda_4(k_8 - \hat{x}_3)Q(S) \tag{3.26}$$

$$\frac{d\lambda_4}{dt} = 0 \tag{3.27}$$

The boundary conditions[+] for these equations, at $t = t_e$, are given by:

$$\begin{aligned} \hat{x}_1(t_e) &= 16.0 \times 10^3 \text{ ft/sec} \\ \hat{x}_3(t_e) &= 30.0 \times 10^4 \text{ ft} \\ \hat{x}_4(t_e) &= 0 \\ \lambda_2(t_e) &= 0 \end{aligned} \tag{3.28}$$

and, at $t = t_f$, are given by:

$$\begin{aligned} \hat{x}_1(t_f) &= v_f \quad \text{ft/sec} \\ \hat{x}_3(t_f) &= 15.0 \times 10^3 \text{ ft} \\ \hat{x}_4(t_f) &= 0 \\ \lambda_2(t_f) &= 0 \ . \end{aligned} \tag{3.29}$$

The otpimal control is of bang-bang type[62] and is given by:

$$\hat{u} = u_o \text{ sgn } (\lambda_2) \ . \tag{3.30}$$

+ In direct re-entry case $\hat{x}_1(t_e) = 26.0 \times 10^3$ ft/sec.

The transversality condition yields:

$$\hat{H}(t_f) = 0 \tag{3.31}$$

where

$$\hat{H} \triangleq \underset{u \in U}{\text{Min}} \; H$$

$$H \triangleq k_9 \, \rho^{\frac{1}{2}} \, x_1^3 + \langle \lambda, \frac{dx}{dt} \rangle$$

The solution of the above TPBVP, if it exists, yields the optimal trajectory, i.e. $\hat{x}$. Unfortunately, it is impossible to apply conventional iterative methods[26,27,28] to solve this TPBVP numerically since the right hand sides of Eqs. (3.20) through (3.27) contain discontinuous terms. Thus, the problem shall be attacked from a different point of view, namely by reconsidering the physical constraints of the problem.

3.3.2 Necessary Conditions for Bounded State Formulation

In neighbouring optimal control solution is sought in the next two sequels by taking advantage of boundedness of one of the state variables. Assume[+] that the optimal trajectory touches the boundary denoted by Eq. (3.16) at least once before it arrives at the target. In other words, assume that there is a trajectory that goes below k_8 and

---

[+] All assumptions will be verified when the open loop optimal trajectory is obtained.

that has less total heat transfer due to convection. This statement is supported by Prichard's results[10] in which the shorter maneuvering time of the capsule in the atmosphere generates less total heat transfer.

Necessary conditions[30] shall be obtained for the state variable when the capsule touches+ the boundary. These conditions (entering corner conditions) are given by the fact that the flight path angle must be zero at such instants. This is due to the fact that the trajectory of $x_2(t)$ must be continuous everywhere in $[t_e, t_f]$. Thus, the conditions are

$$x_2(t_b) = 0 \tag{3.32}$$

$$x_3(t_b) = k_8 \tag{3.33}$$

where $t_b \triangleq$ (the time when the trajectory touches the boundary). It is quite interesting to notice that the above conditions can be also obtained for the problem[30] in which there is no constraint on the control variable but the state variables are bounded such as given by Eq. (3.16). For such a problem, the corresponding corner conditions are:

$$S(t_b) = 0$$

$$\frac{d}{dt} S(t_b) = 0 \quad ,$$

+ The dual valued control $\{+ u_o, - u_o\}$ can not hold the trajectory on the boundary, i.e. the trajectory merely touches the boundary and departs immediately.

which yield the conditions sames as given by Eqs. (3.32) and (3.33).

3.3.3 Closed Loop Solution

In this section, a neighbouring optimal closed loop solution is investigated. Note that the control $u(t)$ when t is in the neighbourhood of t_b should be $+u_o$ (a positive lift), since the trajectory x_3 has to touch the bound from the above. This information — together with the general strategy[16] of spending shorter time in reducing the speed of the capsule in order to have less total heat transfer — gives an inside picture of the optimal control program. That is, the control program should be the one by which, (a) the capsule is brought down to the denser atmosphere as quickly as possible by taking advantage of the higher speed of the capsule at the initial part of the atmospheric re-entry phase, (b) the capsule is pulled up immediately after touching the boundary and then, (c) the capsule is put in a descending maneuver to hit the target.

In order to implement the above strategies, the following control program is proposed: For a shallow initial flight path angle[+], α_e, which is greater than the skip out angle γ_s, let the control be

$$u(t) = u_I(t) = -u_o \tag{3.34}$$

in order to implement the condition (a): Then, let it be switched, at

---

[+] α_e is also bounded from above by γ_c.

$t = t_{s1}$, to

$$u(t) = u_{II}(t) = + u_o \tag{3.35}$$

in order to satisfy the condition (b): Finally, let it be switched, at $t = t_{s2}$, to

$$u(t) = u_{III}(t) = - u_o \ , \tag{3.36}$$

in order to realize the condition[+](c).

The next task is to decide the switching boundaries as functions of state variables. The first switching boundary, denoted by

$$\psi_1(x:k) = 0 \ ,$$

is given by the time independent solution of the system dynamics, i.e. Eqs. (3.12) through (3.14), with the conditions given by Eqs. (3.32), (3.33) and (3.35). The determination of the exact solution is extremely difficult and therefore an approximate solution[++] of the following form is obtained:

[+] Only two switchings would be enough[31] by considering a linear analogue of the problem.

[++] See Appendix B for derivation.

$$\psi_1(x:k) \cong \begin{cases} 1 - \cos x_2 + \dfrac{u_o}{2k_2k_7}\{\rho(x_3) - \rho(k_8)\} \\ \qquad\qquad \text{if } x_3 \le k_{12} \\ 1 - \cos x_2 + \dfrac{u_o}{2k_2}\left\{\dfrac{\rho(k_{12}) - \rho(k_8)}{k_5} + \dfrac{\rho(x_3) - \rho(k_{12})}{k_7}\right\} \\ \qquad\qquad \text{if } x_3 \ge k_{12} \end{cases} \tag{3.37}$$

Similarly, the second switching boundary, denoted by

$$\psi_2(x:k) = 0 \quad ,$$

is given by a time independent solution of the system dynamics, i.e. Eqs. (3.12) through (3.14), with the conditions denoted by Eqs. (3.11) and (3.36). The second order theorem of a re-entry mechanism[5,6,7] is utilized to derive+ an expression such as:

$$\psi_2(x:k) \cong \cos\left\{x_2 + k_2k_7 Z \ln\left(\frac{v_f}{x_1}\right)^2\right\} + \frac{Z}{2}\{\rho(x_3) - \rho(h_f)\} \tag{3.38}$$

where

$$Z \triangleq -\frac{u_o}{2}\frac{1}{k_2k_7} - \frac{\cos x_2}{k_3k_7\rho(x_3)} \cdot \left(\frac{k_1k_3}{x_1^2} - 1\right) \quad .$$

+ See Appendix B for derivation.

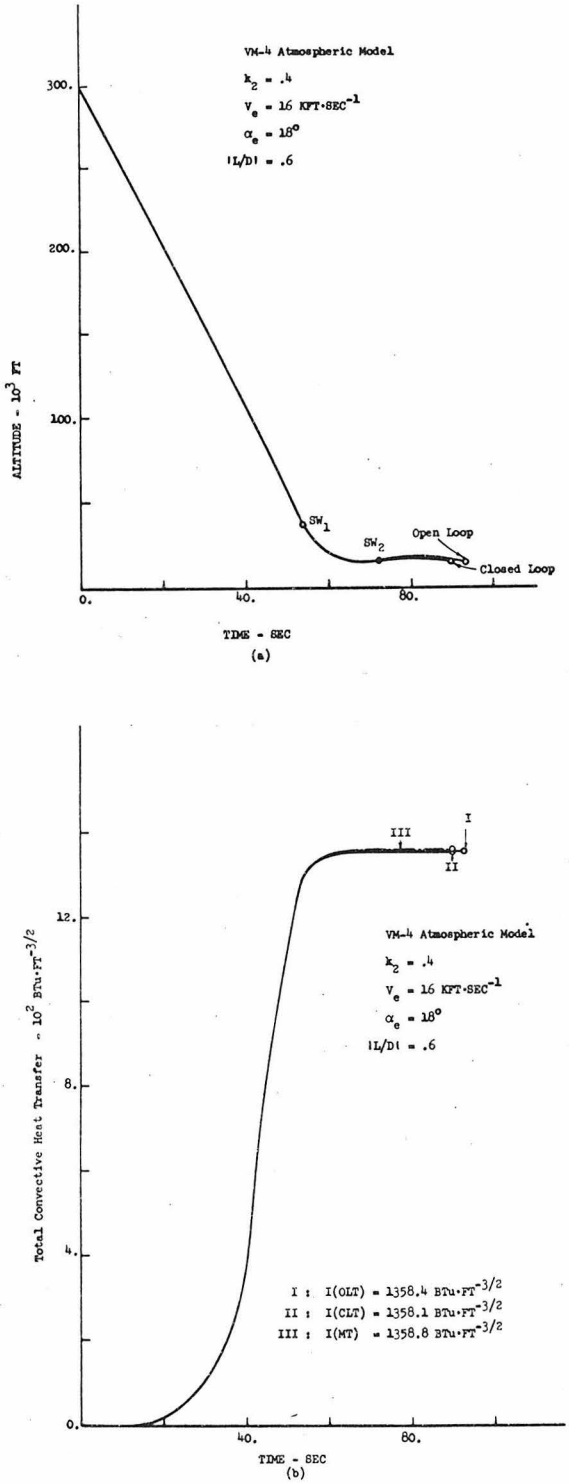

Figure 5. Open loop, closed loop and modified trajectories in orbit re-entry case: (a) Altitude trajectories; (b) performance indeces, I = open loop trajectory, II = closed loop trajectory, III = modified trajectory.

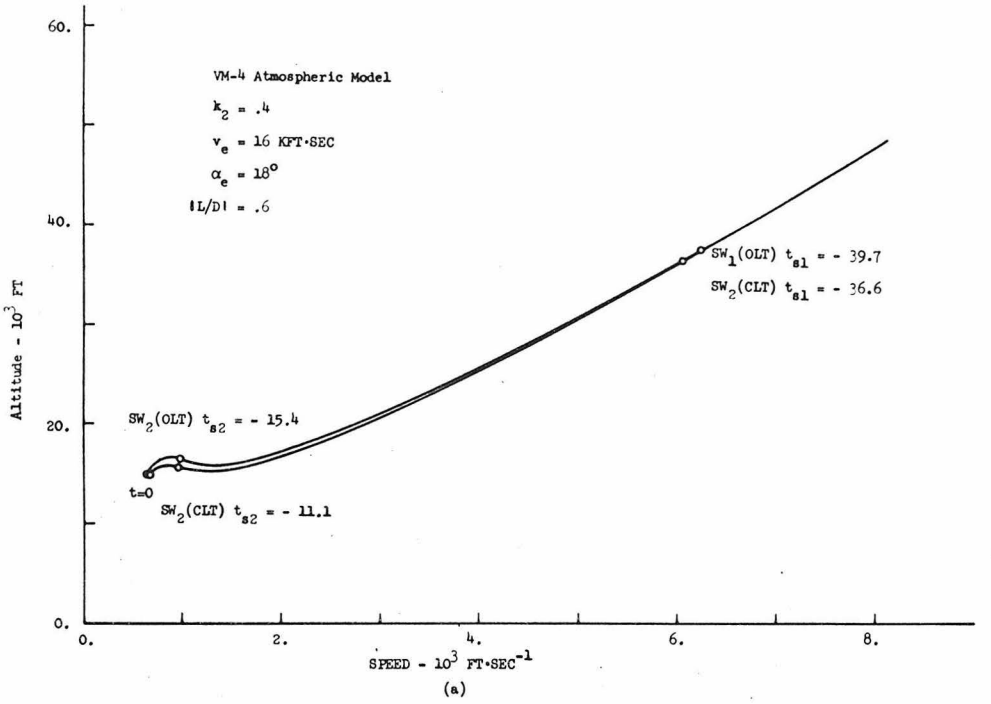

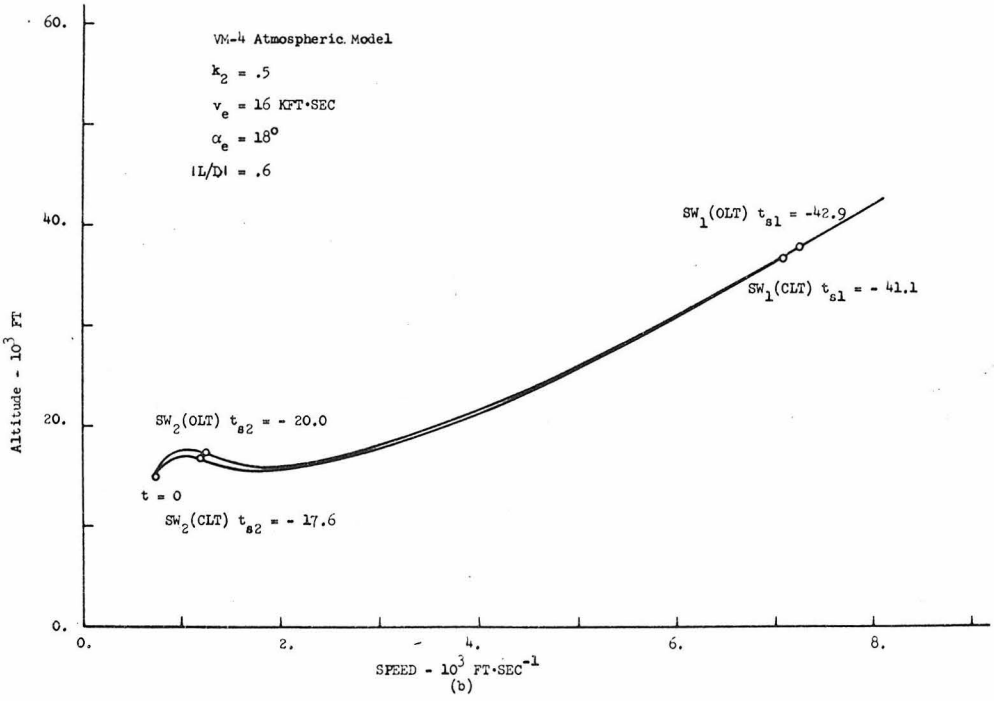

Figure 6. Open loop and closed loop trajectories in the troposphere: (a) Orbit re-entry capsule with $k_2 = 0.4$; (b) Orbit re-entry with $k_2 = 0.5$.

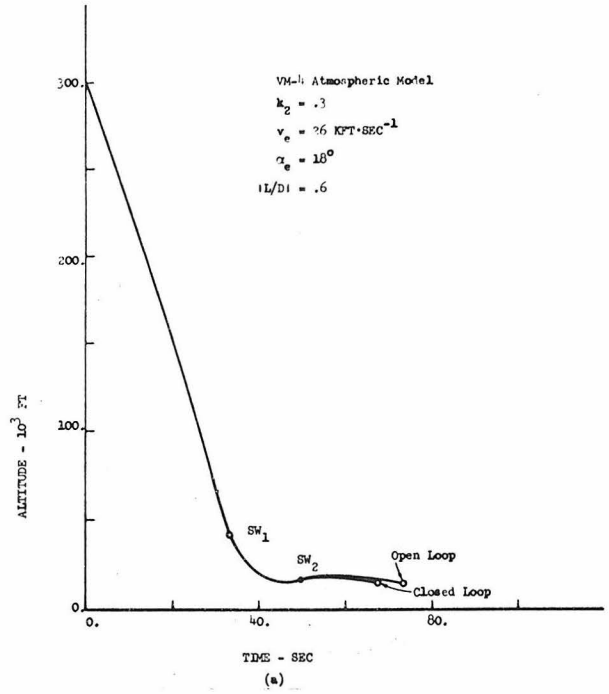

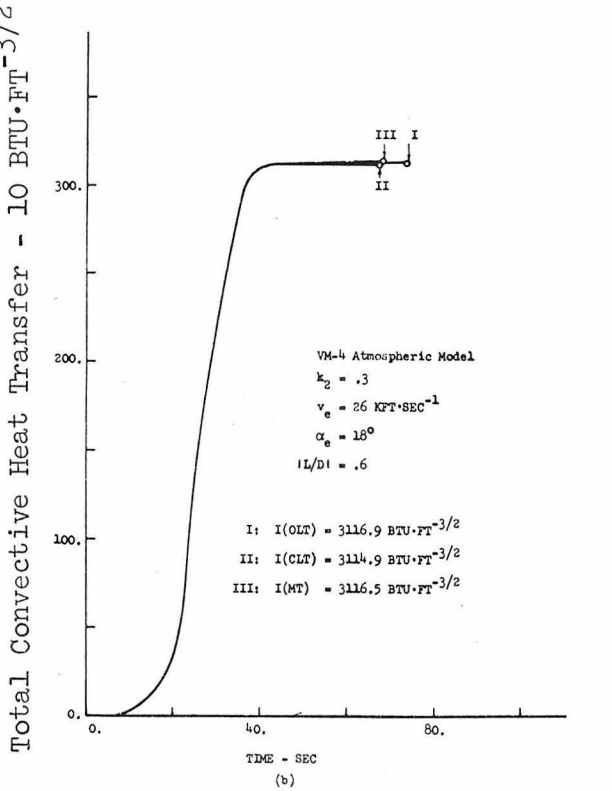

Figure 7. Open loop, closed loop and modified trajectories in direct re-entry case: (a) Altitude trajectories; (b) performance indices, I = open loop trajectory, II = closed loop trajectory, III = modified trajectory.

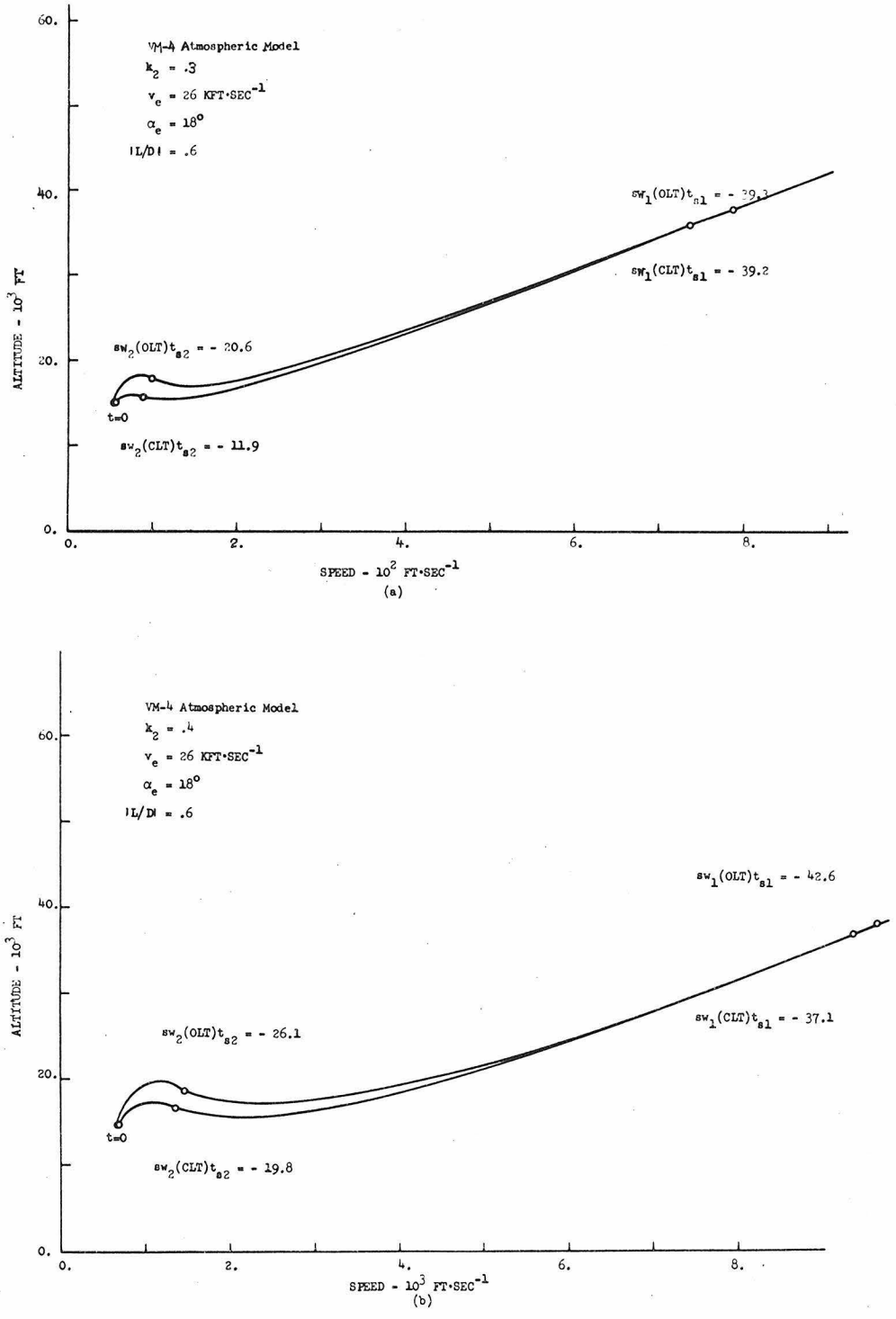

Figure 8. Open loop and closed loop trajectories in the troposphere: (a) Direct re-entry capsule with $k_2 = 0.3$; (b) direct re-entry capsule with $k_2 = 0.4$.

Computer simulation of the re-entry trajectories corresponding to these switching boundaries are illustrated in Figures 5 through 8.

3.3.4 Open Loop Solution

In this section, an open loop solution is studied in order to check the optimality of the closed loop solution. For convenience in the investigation, a particular atmospheric re-entry angle is set such as:

$$x_2(t_o) = \alpha_e = 18 \text{ degrees.} \tag{3.39}$$

A technique which differs somewhat from the conventional iterative methods[26,27,28] is used to solve the TPBVP presented in Section 3.3.1.

Let the canonic equations, i.e. Eqs. (3.20) through (3.27) be rewritten in the following compact form:

$$\frac{d\hat{x}}{dt} = f(\hat{x},\ \text{sgn}(\lambda_2)) \tag{3.40}$$

$$\frac{d\lambda}{dt} = G(\hat{x},\ \text{sgn}(\lambda_2))\ \lambda + h(\hat{x}) \tag{3.41}$$

where $\hat{x} = \text{col}(\hat{x}_1,\ \hat{x}_2,\ \hat{x}_3,\ \hat{x}_4)$

$\lambda = \text{col}(\lambda_1,\ \lambda_2,\ \lambda_3,\ \lambda_4)$.

The boundary conditions for the vector $\hat{x}$ are given, at the initial

point, by Eq. (3.28) with[+]

$$x_2(t_e) = 18 \text{ degrees} \tag{3.39}$$

and, at the terminal point, by Eq. (3.29). Now, the question is how good is the closed loop trajectory, denoted by $x^{(c)}$, as an approximation to the truly optimal trajectory denoted by $\hat{x}$. Here, $x^{(c)}$ is the trajectory generated by the equation such as:

$$\frac{dx^{(c)}}{dt} = f(x^{(c)}, \text{sgn}(\lambda_2^{(c)})) \tag{3.42}$$

where $\lambda_2^{(c)}(t)$ has two zero crossings given by:

$$\lambda_2^{(c)}(t_{s1}) = \lambda_2^{(c)}(t_{s2}) = 0 \ . \tag{3.43}$$

Therefore, if indeed a trajectory of $\lambda^{(c)}$, which is generated by:

$$\frac{d\lambda^{(c)}}{dt} = G(x^{(c)}, \text{sgn}(\lambda_2^{(c)}))\lambda^{(c)} + h(x^{(c)}) \tag{3.44}$$

with conditions (3.43) and

$$\lambda_2^{(c)}(t_f) = 0 \ , \tag{3.45}$$

is obtained, the original TPBVP is completely solved. Since $x^{(c)}$ and $\text{sgn}(\lambda_2^{(c)})$ are known, in Eq. (3.44) G and h are simply known functions of time. Hence, the problem is reduced to the determination

---

[+] Thus, the condition on λ_2 given by Eq. (3.28) must be dropped.

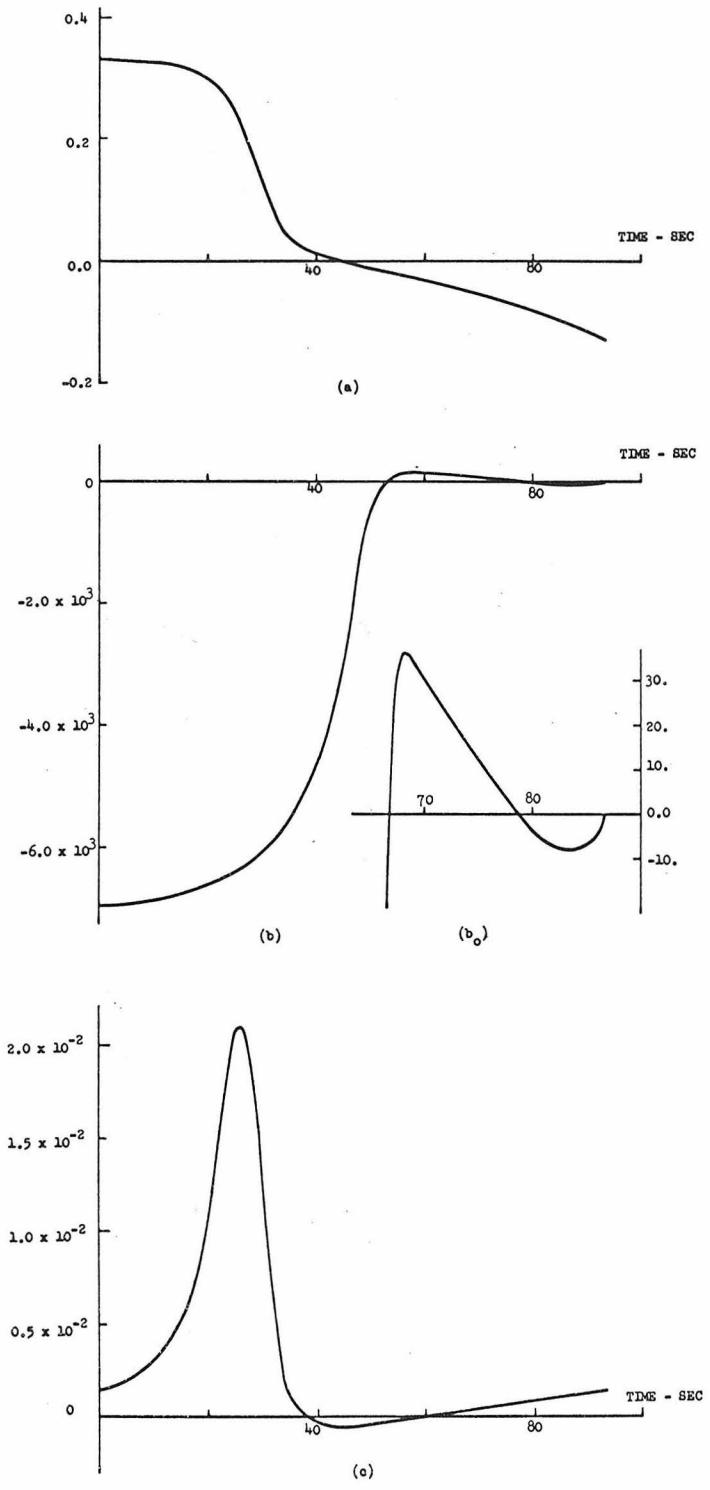

Figure 9. Costate vector, $(\lambda_1, \lambda_2, \lambda_3)$, trajectories.

of a trajectory of $\lambda^{(c)}$ from the differential equation

$$\frac{d\lambda^{(c)}}{dt} = \bar{G}(t)\lambda^{(c)} + \bar{h}(t) \tag{3.46}$$

with the multi points conditions given by Eqs. (3.43) and (3.45) where

$$\bar{G}(t) \triangleq G(x^{(c)}, \text{sgn}(\lambda_2^{(c)}))$$

$$\bar{h}(t) = h(x^{(c)}) \quad .$$

This is a linear multi point boundary problem, which can be solved easily. A numerical experiment has been performed to check if indeed

$$\hat{H}(t) = 0 \tag{3.47}$$

is satisfied for $\forall t \in [t_e, t_f]$, where t_f is assumed to be the time when the trajectory $x^{(c)}$ hits the target. A set of trajectories of λ so generated are shown in Figure 9. Small adjustments of switching times are required. The resulting trajectories and performance indices are depicted in Figures 5 through 8. For both direct and orbit re-entry schemes, the closed loop trajectories obtained before are proven to be neighbouring optimal trajectories.

3.3.5 Modification of the Solution

Due to approximations in obtaining the switching boundaries ψ_1 and ψ_2, the capsule cannot hit the target with the exact speed which is expected. The deviation in speed becomes significant when the extreme atmospheric models, i.e. VM-8 and VM-10, are assumed. In order

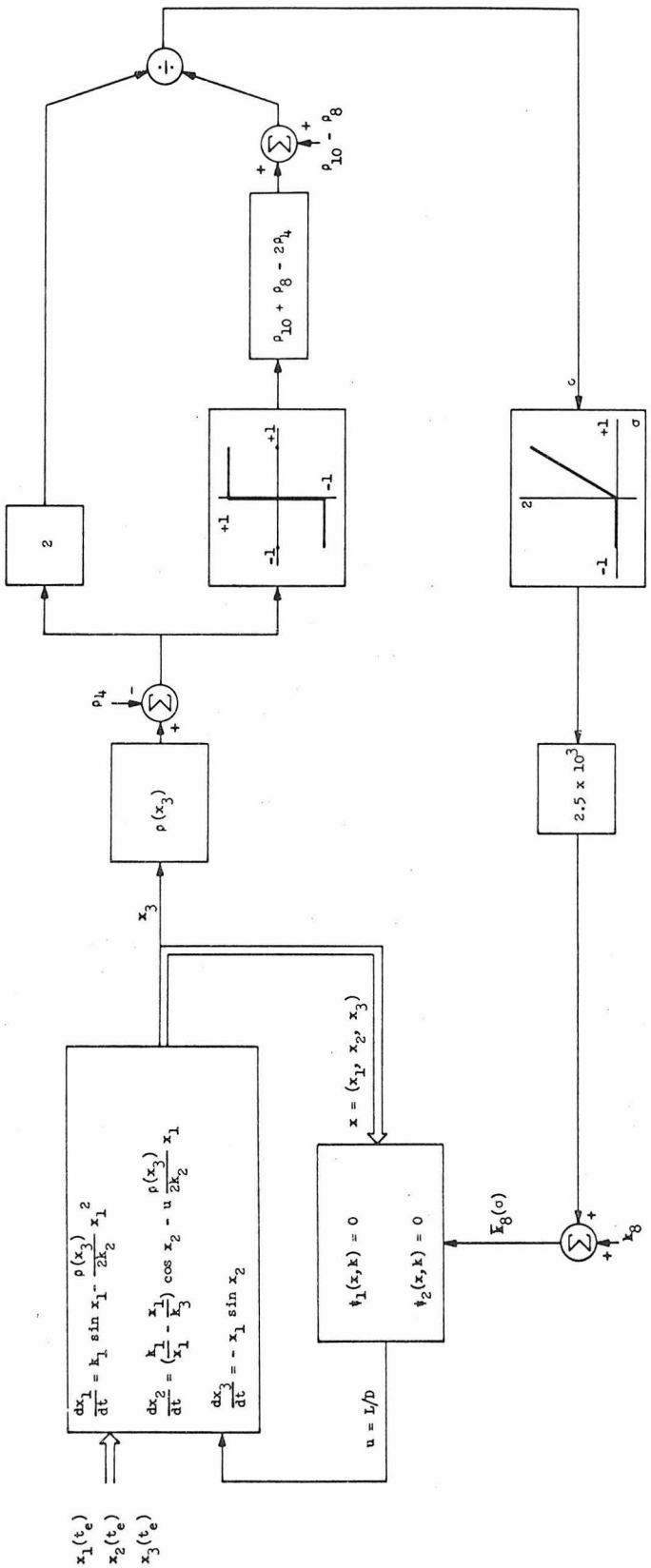

Figure 10. Complete deterministic control system block diagram.

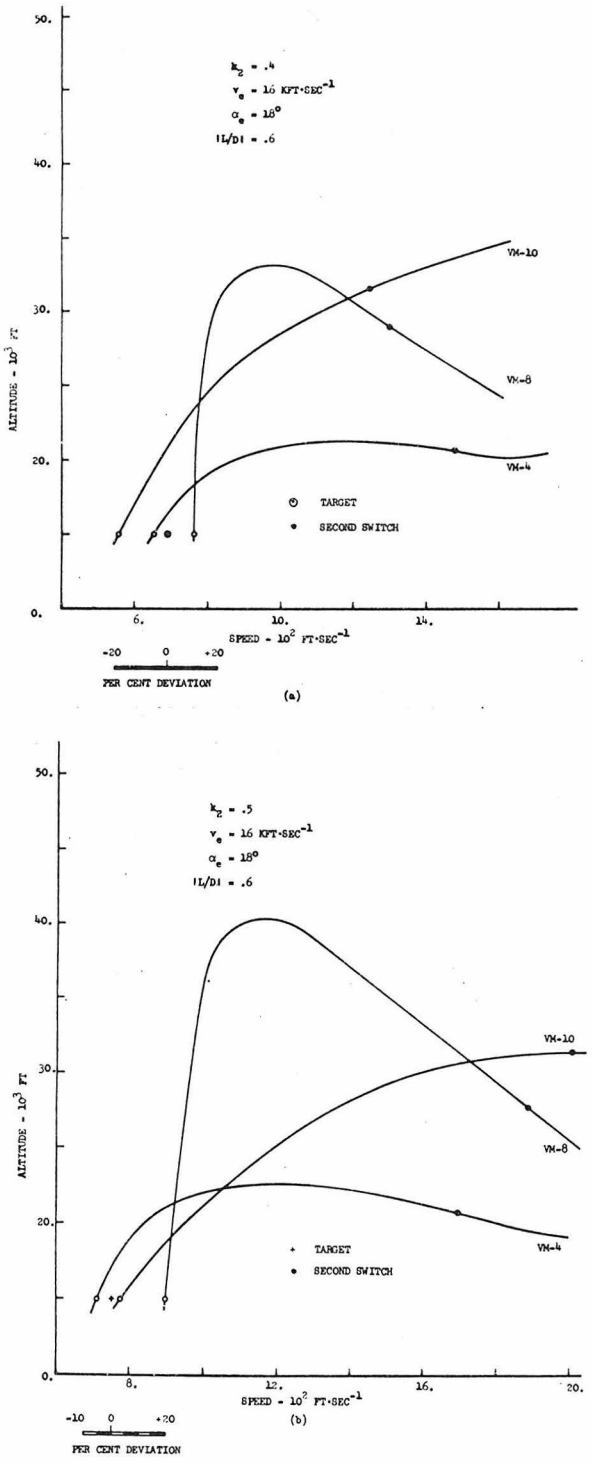

Figure 11. Modified trajectories near target:
(a) Orbit re-entry with $k_2 = 0.4$;
(b) orbit re-entry with $k_2 = 0.5$.

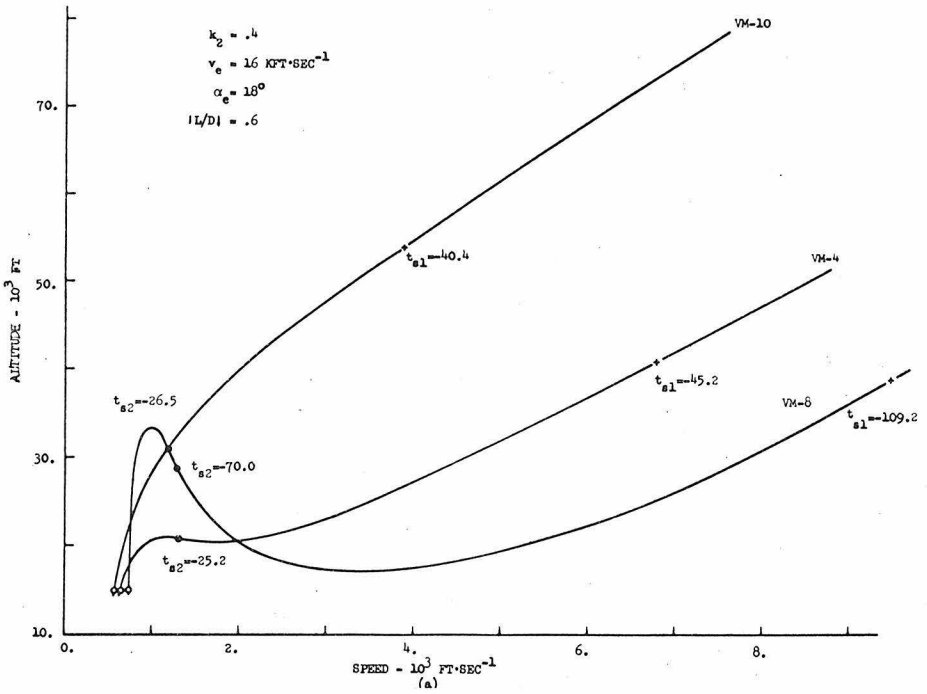

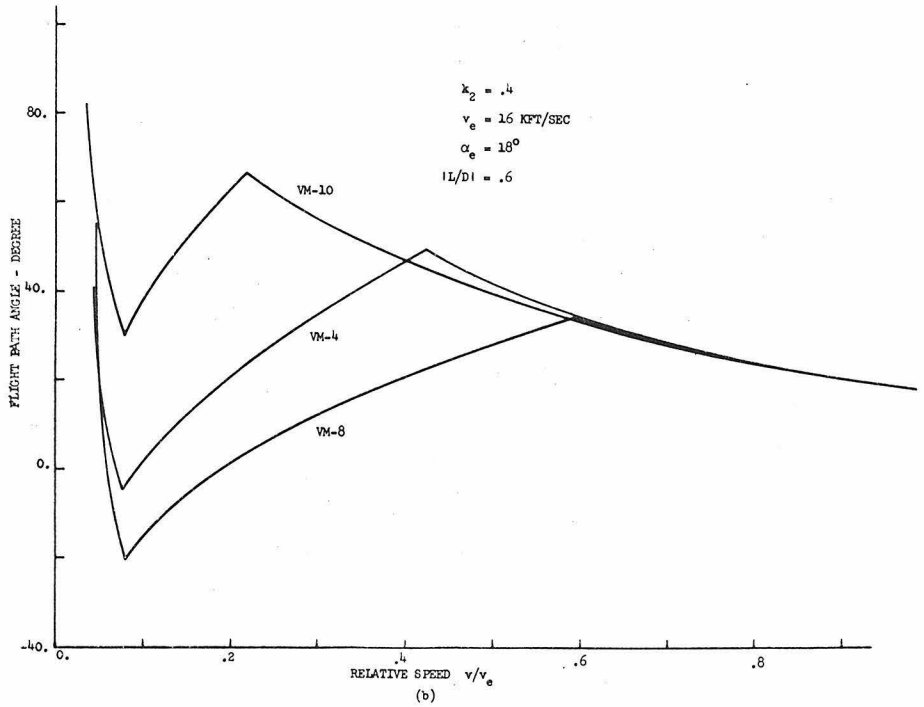

Figure 12. Modified trajectories in the troposphere:
(a) Altitude versus speed, $k_2 = 0.4$;
(b) flight path angle versus speed, $k_2 = 0.4$.

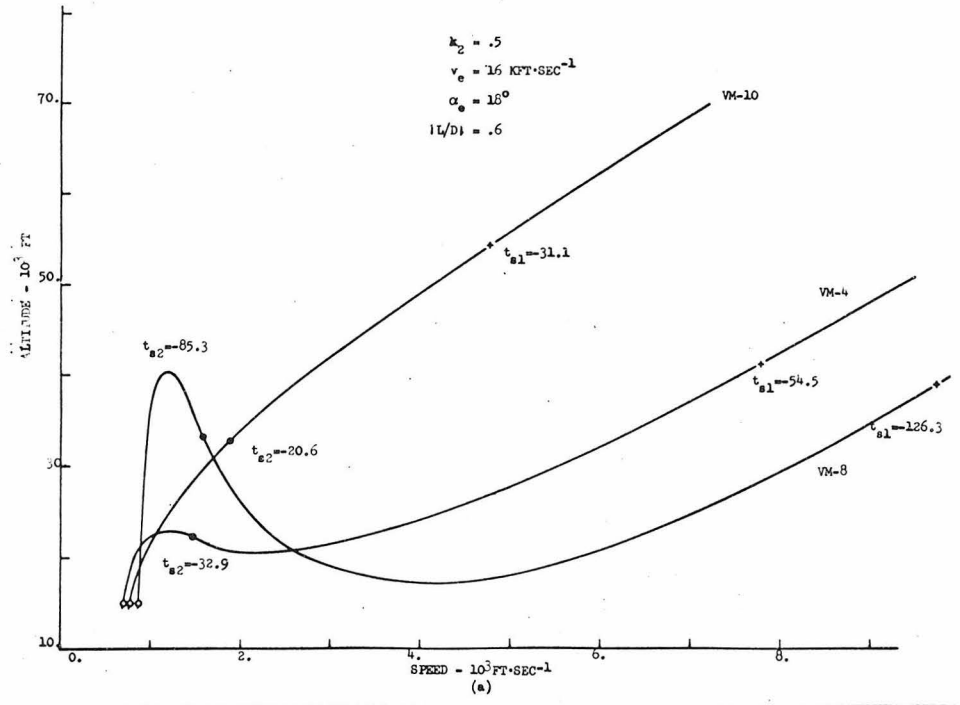

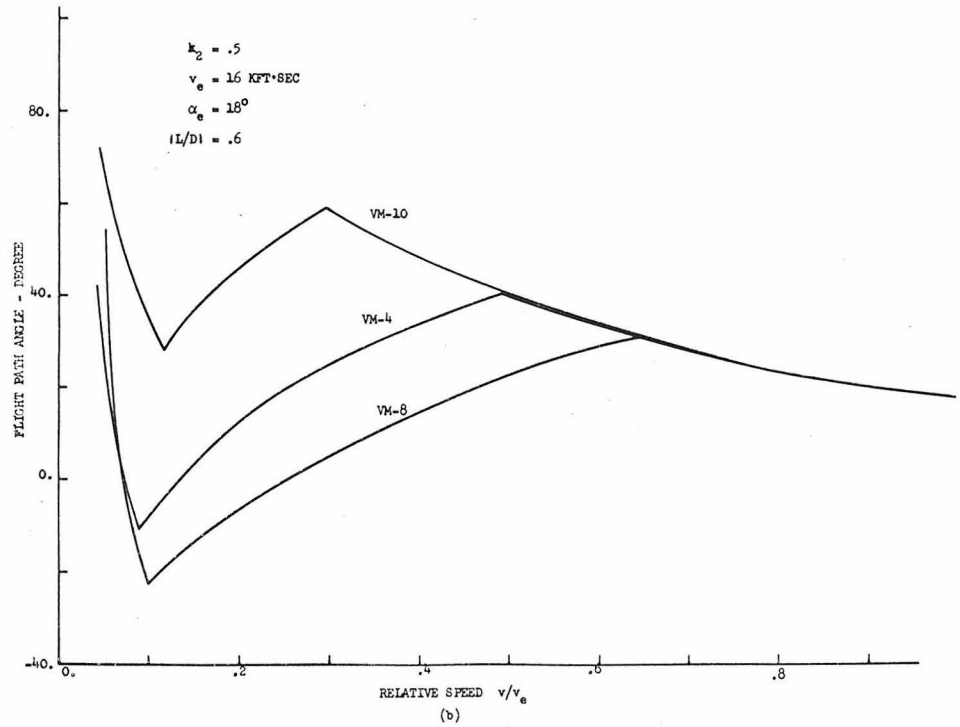

Figure 13. Modified trajectories in the troposphere: (a) Altitude versus speed, $k_2 = 0.5$; (b) flight path angle versus speed, $k_2 = 0.5$.

to circumvent this difficulty, the parameter k_8 is modified to be $\bar{k}_8$ where

$$\bar{k}_8(\sigma) \triangleq k_8 + 2.5 \times 10^3(\sigma - |\sigma|) \tag{3.48}$$

$$\sigma \triangleq \frac{2(\rho - \rho_4)}{\rho_{10} - \rho_8 + (\rho_{10} + \rho_8 - 2\rho_4)\ \mathrm{sgn}(\rho - \rho_4)} \tag{3.49}$$

$\rho_N \triangleq$ VM-N atmospheric density model

$\rho \triangleq$ any atmospheric density model between VM-8 and VM-10 .

By performing this modification, the deviation in speed is improved and is less than 15 per cent of the desired value. Such trajectories+ near the target are depicted in Figures 11 through 13. The block diagram of the control system is illustrated in Figure 10. Implementation of such a control system by utilizing an on board computer with suitable size and speed is within the grasp of modern technology.

3.4 Discussions

3.4.1 A Relation to the Minimum Time Trajectory

The performance index of the minimum heat generation problem given by:

$$I(u) = \int_{t_e}^{t_f} k_9\ \rho^{\frac{1}{2}}(x_3)\ x_1^3 dt \tag{3.50}$$

+ These trajectories also satisfy the terminal conditions:

$x_2(t_f) \geq 45$ degrees

to ensure the radar observation[13,16] in the soft landing phase for a Voyager type capsule.[18]

is a monotone increasing function of time t_f. But it is not apparent that the minimum time problem, where the performance index is given by

$$J(u) = \int_{t_e}^{t_f} dt \quad , \tag{3.51}$$

implies that the heat generation is minimized. The relationship between these two problems is investigated with the assumption that they have unique optimal solutions.

Let

$$\mu \triangleq \text{col}\ (\mu_1, \mu_2, \mu_3, \mu_4)$$

be the costate vector in the minimum time problem. Let the re-entry dynamics be subject to the same conditions as discussed in the minimum heat generation problem. That is, the dynamical equations of motion of the capsule are given by:

$$\frac{dx_1}{dt} = k_1 \sin x_2 - \frac{\rho(x_3)x_1^2}{2k_2} \tag{3.51}$$

$$\frac{dx_2}{dt} = \left(\frac{k_1}{x_1} - \frac{x_1}{k_3}\right) \cos x_2 - u \frac{\rho(x_3)x_1}{2k_2} \tag{3.52}$$

$$\frac{dx_3}{dt} = - x_1 \sin x_2 \tag{3.53}$$

$$\frac{dx_4}{dt} = Q(S)\ (k_8 - x_3)^2 \quad . \tag{3.54}$$

Let $\tilde{x}$ denote the time optimal trajectory. Let the canonic equations in the minimum time problem be designated in the following compact form:

$$\frac{dx}{dt} = f(\tilde{x},\ \mathrm{sgn}(\mu_2):\ k) \tag{3.55}$$

$$\frac{d\mu}{dt} = G(\tilde{x},\ \mathrm{sgn}(\mu_2):\ k)\ \mu \quad . \tag{3.56}$$

Then, the canonic equations in the minimum heat generation problem are given by:

$$\frac{d\hat{x}}{dt} = f\ (\hat{x},\ \mathrm{sgn}(\lambda_2):\ k) \tag{3.57}$$

$$\frac{d\lambda}{dt} = G(\hat{x},\ \mathrm{sgn}(\lambda_2):k)$$

$$+\ \mathrm{col}\ (-\ 3k_9\rho^{\frac{1}{2}}(\hat{x}_3)\hat{x}_1^{\,2},\ 0,\ \frac{k_5k_9}{2}\ \rho^{\frac{1}{2}}(\hat{x}_3)\hat{x}_1^{\,3},0) \tag{3.58}$$

Observe that $(\hat{x},\ \tilde{x})$, $(\lambda_2,\ \mu_2)$ and $(\lambda_4,\ \mu_4)$ equations are form invariant. The boundary conditions on $\tilde{x}$ are the same as those of $\hat{x}$. Similarly, the boundary conditions on λ and μ are given by:

$$\lambda_2(t_e) = \lambda_2(t_f) = 0 \tag{3.59}$$

$$\mu_2(t_e) = \mu_2(t_f) = 0 \quad . \tag{3.60}$$

Therefore, if a form invariance can be shown among equations of $(\mu_1,\ \lambda_1)$ and $(\mu_3,\ \lambda_3)$, then the trajectories of λ_2 and μ_2 are the

same. This is proved as follows: Consider a sequence of minimum heat generation problems in which the performance indices, $\{I^{(n)}(u),\ n = o, 1, \ldots\}$, are given by:

$$I^{(n)}(u) = \int_{t_e}^{t_f} k_9^{(n)}\ \rho^{\frac{1}{2}}(x_3)\ x_1^3\ dt \tag{3.61}$$

where the sequence $\{k_9^{(n)}\}$ is positive monotone decreasing to zero, with

$$k_9^{(o)} = k_9 \ . \tag{3.62}$$

It will be shown that the optimal control laws in the sequence of the problems are the same, i.e. independent of $k_9^{(n)}$'s. Let $\hat{u}^{(n+1)}$ and $\hat{u}^{(n)}$ be the optimal control law in $(n + 1)$st and n-th problems, respectively. Then, it is apparent that

$$\hat{u}^{(n+1)} \equiv \hat{u}^{(n)} \tag{3.63}$$

since

$$\begin{aligned} &\min_u I^{(n+1)}(u) \quad (= I^{(n+1)}(\hat{u}^{(n+1)})) \\ &= \min_u \frac{k_9^{(n+1)}}{k_9^{(n)}}\ I^{(n)}(u) \\ &= \frac{k_9^{(n+1)}}{k_9^{(n)}}\ \min_u I^{(n)}(u) \end{aligned}$$

$$= \frac{k_9^{(n+1)}}{k_9^{(n)}} \quad I^{(n)}(\hat{u}^{(n)}) \tag{3.64}$$

A mathematical induction can be used to generalize this argument for $\forall\ n = 0, 1, 2, \ldots$. Therefore, the control law corresponding to the performance index with $k_9^{(o)} (= k_9)$ is equivalent to that with $k_9^{(\infty)}$. But the sequence, $\{k_9^{(n)}\}$, has been assumed to be

$$\lim_{n\to\infty} k_9^{(n)} = 0 \quad . \tag{3.65}$$

Hence, from Eqs. (3.55) through (3.60), it can be concluded that

$$\mu_2(t) \equiv \lambda_2(t) \tag{3.66}$$

for $\forall\ t \in [t_e, t_f]$. Therefore, if the minimum time and minimum heat generation problems have unique optimal solutions. Then the optimal trajectories for these two problems are identical.

3.4.2 Instantaneous Heat Generation

A simple relation between instantaneous heat generation and the atmospheric density is derived. This relation holds for any atmospheric density model as well as for any re-entry trajectory.

Eq. (3.51) is multiplied by $k_9 x_1$ to yield an equation such as:

$$\rho^{\frac{1}{2}} q_c = 2k_2 k_9 [x_1 \frac{dx_1}{dt} - k_1 x_1 \sin x_2] \tag{3.67}$$

where

$$q_c \triangleq k_9 \rho^{\frac{1}{2}}(x_3)\, x_1^3$$

= (instantaneous heat generation due to convection).

Substitution of Eq. (3.53) into Eq. (3.67), and integration of the resulting equation leads to an expression of the following form:

$$\int_{t_e}^{t_f} \rho^{\frac{1}{2}} q_c \, dt$$

$$= \frac{2k_2k_8}{m}\left[\frac{m}{2}\{x_1^2(t_e)-x_1^2(t_f)\} + mk_1\{x_3(t_e) - x_3(t_f)\}\right] \tag{3.68}$$

where $m \triangleq$ mass of the capsule. The quantity within the square bracket is the difference (at the beginning and at the end of the atmospheric re-entry phase) of the total energy of the capsule. Hence, as soon as the initial condition and the target of the atmospheric re-entry phase are specified, there exists a simple relation between the atmospheric density and the instantaneous heat generation of the form

$$\int_{t_e}^{t_f} \rho^{\frac{1}{2}} q_c \, dt = \text{constant} \quad , \tag{3.69}$$

irrespective to the kind of trajectory taken.

3.4.3 Conclusive Remarks

Quantities related to the performance index are tabulated in Table 2. Improvements made on these quantities in comparison with a

TABLE 2. Comparison of variable lift to drag ratio control re-entry scheme with ballistic re-entry scheme.

	Dimension	VM-4	VM-8	VM-10
Max. Instantaneous Heat Generation	$BTU/ft^{3/2} \cdot sec$	76.5 (78.0)†	65.2 (67.9)	78.8 (79.1)
Total Heat Generation	$BTU/ft^{3/2}$	1358.8 (1467.0)	1406.9 (1638.7)	1507.3 (1510.0)
Time Spent for Re-entry	sec	98.4 (157.7)	162.9 (182.4)	80.3 (127.4)
Distance Traversed	mile	157.7	182.4	127.4

†The quantities inside the brackets are the corresponding values of a ballistic re-entry when the same initial conditions are assumed.

ballistic re-entry scheme are not significant. However, the variable lift to drag ratio control scheme should not be evaluated from this table only.

The prime innovation of this scheme is that the terminal speed of the capsule can be controlled at all times regardless of the possible atmospheric environment of Mars. This cannot be achieved by a ballistic re-entry scheme or by a constant lift to drag ratio re-entry scheme. The entry angle corridor has been widened to the range of 14 degrees to 34 degrees. This is due to the fact that the control force in the beginning of the atmospheric re-entry phase is always negative. Although the ballistic constant has been fixed at a particular value, the control scheme is still feasible for a range of values of the ballistic constant by changing the value of lift to drag ratio.

Improvement of the off target deviation can be achieved by performing better approximation in the determination of the second switching boundary, even though an exact solution is almost impossible. Although a series solution of the re-entry mechanics is reported,[7] it seems doubtful that it can be used instead of Eq. (3.38) because of the complexity of such a solution.

IV. ESTIMATION OF SYSTEM PARAMETER

4.1 Introduction

It has been shown that the gliding re-entry trajectory solely depends upon the characteristics of the Martian atmosphere. Better understanding of the physical characteristics of Martian atmosphere has engaged the attention of scientists[14] from the beginning of this century. Until quite recently, the Martian atmospheric pressure at ground level had been believed[24] to be around 20 mb. The successful missions of Mariner IV in 1964 and the Mariner V in 1967 brought a large amount of scientific data about the atmospheric conditions around Mars. The Mariners' data indicates that the atmospheric pressure is somewhere in the range from 5 mb to 10 mb. NASA and JPL are proposing[14,18] ten different atmospheric density models of Mars. The parameter values of these models are still scattered over a wide range.

One of the tasks posed upon the control system is, therefore, to identify the parameter values of the Martian atmosphere during the atmospheric re-entry phase of the capsule. Moreover, identification of the Martian atmospheric parameters and estimation of the state vector must be performed on line in real time based upon the observations at each instant of time. A nonlinear filter is developed to accomplish this task before the capsule arrives at an altitude of $100. \times 10^3$ ft. Above this altitude the Martian atmosphere is assumed[18] to be stationary. If indeed the system identification can be done before the Martian atmosphere poses stochastic behaviour, then a stochastic optimal control problem can be handled independently. This, in turn, prevents the problem to be buried in the mist of complexity.

It is shown that the inertial observation is the only information available on the flight path if a Voyager type capsule[18] is employed. The sequential estimator by Detchmendy and Sridhar[44] is utilized since this filter does not require any particular statistical assumption+ of the plant dynamics or of the observations.

4.2 Inertial Observations

The flight path of the capsule in the approach phase as well as in the atmospheric re-entry phase can be obtained by inertial observations. This section is concerned with the error analysis of inertial observations initiated by the orbit determination.

Errors in the inertial observations are caused by asymptotic errors of the orbit determination,[20,21] gyro measurement errors[34,35] at bus and capsule separation and the dynamical errors in accelerometers. The first two give rise to biased noise, and the last results in random noise in the inertial observations.

It is known[21] that the errors in orbit determination++ are as much as:

$$\frac{|\delta T_p|}{T_p} \leq 3.0 \times 10^{-7} \tag{4.1}$$

$$\frac{|\delta x_3|}{x_3} \leq 5.5 \times 10^{-4} \tag{4.2}$$

+ See Section 5.5.2 for further discussions.

++ It takes about 50 hours to attain this much accuracy.

if they are performed by celestial observations with on board instruments. For simplicity, let a perfect circle in a plane be assumed for the parking orbit of the capsule. Then, the error in determination of the velocity is given by:

$$\frac{|\delta x_1|}{x_1} \leq \frac{|\delta x_3|}{x_3}\frac{x_3}{k_3} + \frac{\delta T_p}{T_p} = 3.96 \times 10^{-5} \tag{4.3}$$

It is also known[63] that the total gyro drift caused by the separation shock impulse is less than 0.05 degrees in the measurement of the flight path angle. Therefore, the angular error immediately after the separation is as much as:

$$\frac{|\delta x_2|}{x_2} \leq 3.1 \times 10^{-3} \tag{4.4}$$

if the nominal flight path angle after separation is assumed to be 18 degrees.

Dynamical errors of the accelerometers are analyzed as follows: Assume the accelerometers are fixed along the horizontal and vertical axes. Then, the magnitude of the dynamical errors δV_x and δV_y of these accelerometers are given[34,35] by:

$$\frac{d}{dt}(\delta V_x) = \sum_{i=o}^{3} N_{ix}\left(\frac{dV_x}{dt}\right)^i + \sum_{i=o}^{1} M_{ix}\left(\frac{dV_x}{dt}\right)^i\left(\frac{dV_y}{dt}\right)$$

$$\frac{d}{dt}(\delta V_y) = \sum_{i=o}^{3} N_{iy}\left(\frac{dV_y}{dt}\right)^i + \sum_{i=o}^{1} M_{iy}\left(\frac{dV_y}{dt}\right)^i\left(\frac{dV_x}{dt}\right) \tag{4.5}$$

where

N_o, M_o $\triangleq$ error coefficients due to bias shift,

N_1, M_1 $\triangleq$ error coefficients due to scale factor and,

N_2, N_3 $\triangleq$ error coefficients due to nonlinearity of gauges.

Thus, the inertial observations denoted by

$$y = \text{col}\ (y_1,\ y_2,\ y_3)$$

can be simulated by the following equations:

$$\frac{dy_1}{dt} = \frac{V_x\left(\frac{dV_x}{dt}\right) + V_y\left(\frac{dV_y}{dt}\right)}{V_x^2 + V_y^2} \tag{4.6}$$

$$\frac{dy_2}{dt} = \left(\frac{k_1}{y_1} - \frac{y_1}{k_3}\right) \cos y_2 - \left(\frac{L}{D}\right) \frac{\rho(y_3)y_1}{2k_2} \tag{4.7}$$

$$\frac{dy_3}{dt} = - V_y \tag{4.8}$$

where

$$\frac{dV_x}{dt} = \frac{d}{dt}(x_1 \cos x_2) + Z_x(t) \cdot \frac{d}{dt}(\delta V_x) \tag{4.9}$$

$$\frac{dV_y}{dt} = \frac{d}{dt}(x_1 \sin x_2) + Z_y(t) \cdot \frac{d}{dt}(\delta V_y) \tag{4.10}$$

Z_x, Z_y $\triangleq$ Gaussian processes with zero mean and unit variance.

The initial conditions of y for the worst case are given by:

$$y(t_{do}) = [I + \delta X]\ x(t_{do}) \tag{4.11}$$

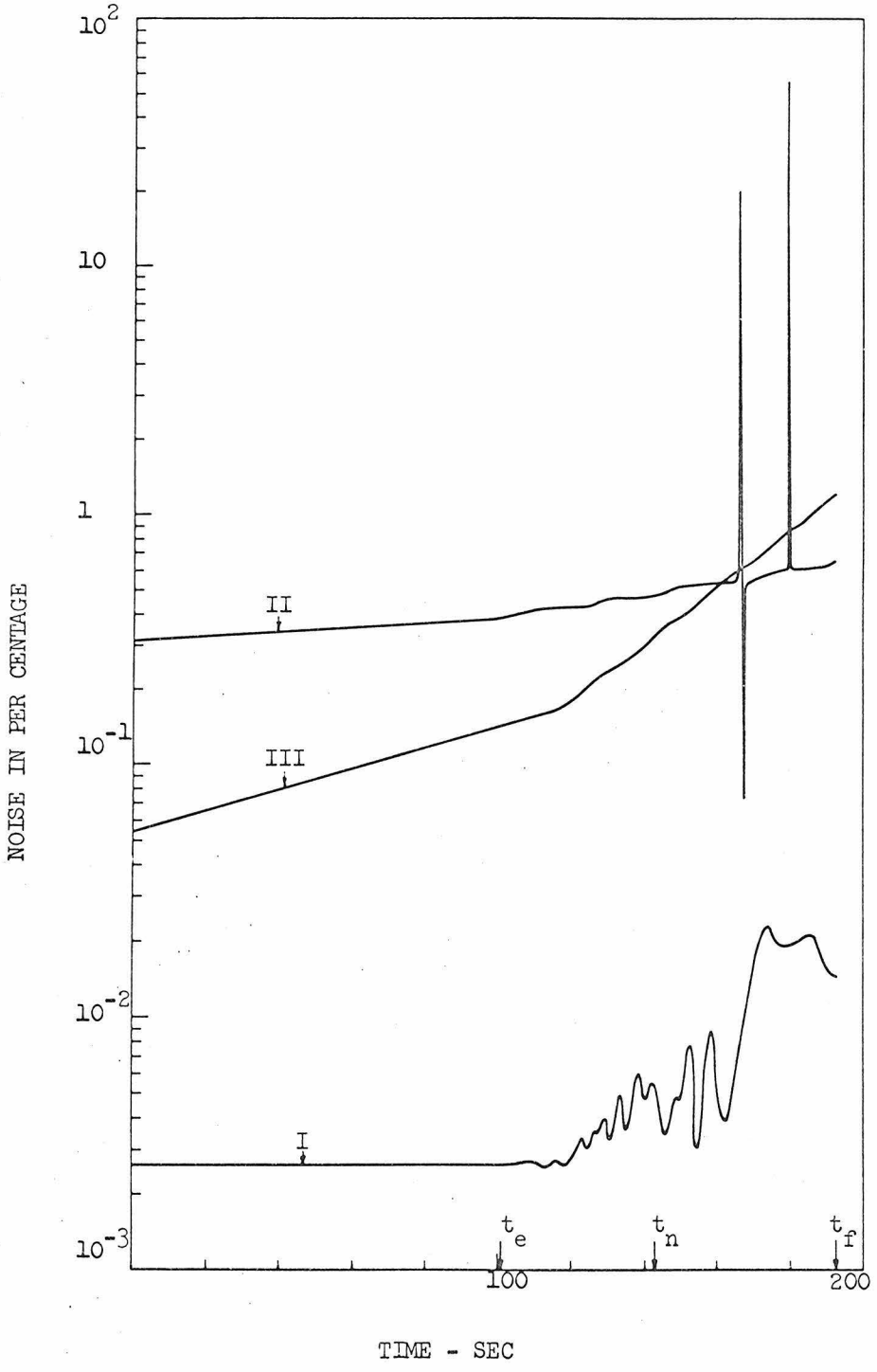

Figure 14. Typical noise of inertial observation: I = noise in speed data; II = noise in flight path angle data; III = noise in altitude data.

where

$$\delta X = \begin{cases} \delta x_i & \text{if } i = j \\ 0 & \text{otherwise} \end{cases} .$$

Typical sample functions of the observational noise processes, denoted by η, are illustrated in Figure 14, where the inertial observation is characterized by

$$y_i = x_i + \eta_i \qquad (4.12)$$

$$i \in (1, 2, 3)$$

where it is seen that the above noise processes are biased and correlated.

4.3 Nonlinear Filter

4.3.1 Formulation of the Problem

This section is concerned with the refinement of the inertially observed flight path data and estimation of a parameter associated with the atmospheric density models. It is a natural assumption that the altitude gradient parameters k_5 and k_7 of the atmospheric density models are known from Figure 2. On the other hand, the surface density parameter[+] k_4 must be identified as the capsule descends into the Martian atmosphere. This is accomplished by treating the parameter as one of the state variables. Thus, the system dynamics should be re-

---

[+] The corresponding parameter k_6 in the troposphere can be known through a relation such as

$$k_6 = 0.18\, k_4 \quad .$$

written as:

$$\frac{dx_1}{dt} = k_1 \sin x_2 - \frac{1}{2k_2} x_1^2 x_4 \exp[-k_5 x_3] \tag{4.13}$$

$$\frac{dx_2}{dt} = \left(\frac{k_1}{x_1} - \frac{x_1}{k_3}\right) \cos x_2 - \frac{\hat{u}}{2k_2} x_1 x_4 \exp[-k_5 x_3] \tag{4.14}$$

$$\frac{dx_3}{dt} = - x_1 \sin x_2 \tag{4.15}$$

$$\frac{dx_4}{dt} = 0 \tag{4.16}$$

It should be noticed that estimation of the parameter k_4 should be performed before the capsule arrives at the altitudes of $100. \times 10^3$ ft. This implies that the control law is given by:

$$\hat{u} = - u_o$$

throughout the estimation period.

Let the dynamical system, i.e. Eqs. (4.13) through (4.16), be expressed in a compact form

$$\frac{dx}{dt} = f(x, \hat{u}; k) \tag{4.17}$$

Let $\epsilon_1(t)$ and $\epsilon_2(t)$ be vector valued residual errors defined by:

$$\epsilon_1(t) \triangleq y - \bar{x} \tag{4.18}$$

$$\epsilon_2(t) \triangleq \dot{\bar{x}} - f(\bar{x}, \hat{u}; k) \tag{4.19}$$

where

$\bar{x} \triangleq$ (any estimate of the vector x).

Then, the best estimate μ of the vector x is defined as the one that minimizes the cumulative error such as:

$$\|x(t_e) - \mu_e\|^2_{P_o^{-1}} + \int_{t_e}^{t} \{\|\epsilon_1(\tau)\|^2_{Q(\tau)} + \|\epsilon_2(\tau)\|^2_{P(\tau)}\}\, d\tau \qquad (4.20)$$

for each instant of time, where

$\mu_e \triangleq$ a-priori knowledge of $x(t_e)$

$\|\cdot\|_P \triangleq$ a Euclidean semi-norm

P & Q $\triangleq$ semi positive and positive definite matrices, respectively. The estimation problem has been completely formulated as a variational problem. Another significant point of this approach is that no statistical assumption is required[44] about the unknown elements of the plant dynamics or the observations.

4.3.2 Sequential Estimator

Let the observations (4.12) be denoted in a compact form as:

$$y = H x + \eta \qquad (4.21)$$

where $H \triangleq (I_{33} \vdots 0_{31})$.

Then, the best estimate μ of the vector x is given+ by the following vector and matrix equations:

+ For the details of derivations, see the reference [44] etc.

$$\frac{d\mu}{dt} = f(\mu,\ \hat{u};\ k) + 2\Gamma H^{*}Q(y - H\mu) \tag{4.22}$$

$$\frac{d\Gamma}{dt} = \frac{P}{2} + \Gamma\left(\frac{\partial f}{\partial x}\right)^{*}_{x=\mu} + \left(\frac{\partial f}{\partial x}\right)_{x=\mu}\Gamma - \Gamma H Q H^{*}\Gamma \tag{4.23}$$

The initial conditions on these equations are given by:

$$\mu(t_e) = \mu_e \tag{4.24}$$

$$T(t_e) = P_o \tag{4.25}$$

It is noted that Eq. (4.23) is independent of the observation y. Indeed Eqs. (4.22) and (4.23) constitute an approximation of an exact nonlinear filter,[+] and are interpreted[45] as follows: Eq. (4.22) is an approximation of the mean of the random variable x conditioned on the past observations. Similarly, Eq. (4.23) is an approximation to the second moment of such random variable x.

4.3.3 Simulations

A numerical experiment is necessary in order to verify the goodness of the approximation. The basic requirement of this filter is whether or not estimation of the state $x_4 (= k_4)$ can be accomplished within the desired time period. On the other hand, refinement of the flight path data is an easy task[++] for the filter. This is because the flight path of the capsule can be observed by the on board instruments with a reasonably small amount of error. Figure 15 illustrates

---

+ Kushner equation.[46,65]

++ An improvement by the factor of 10, in signal to noise ratio, has been accomplished.

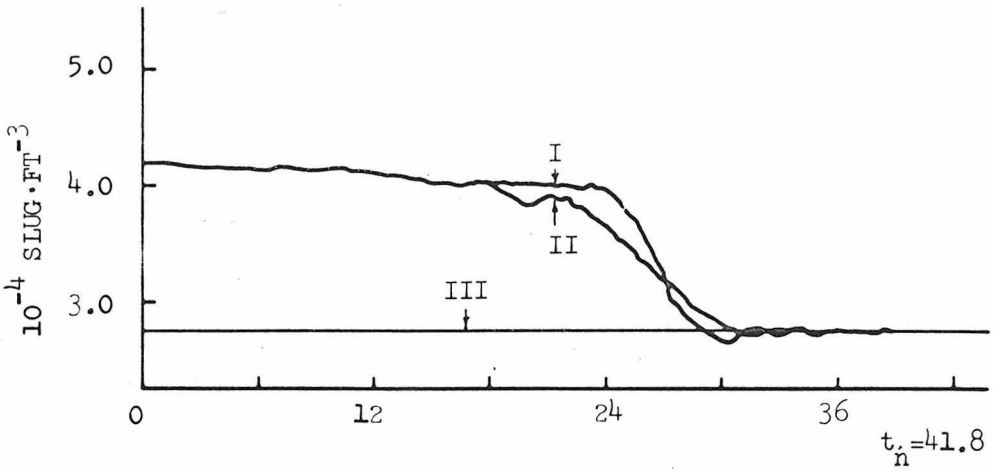

(a)

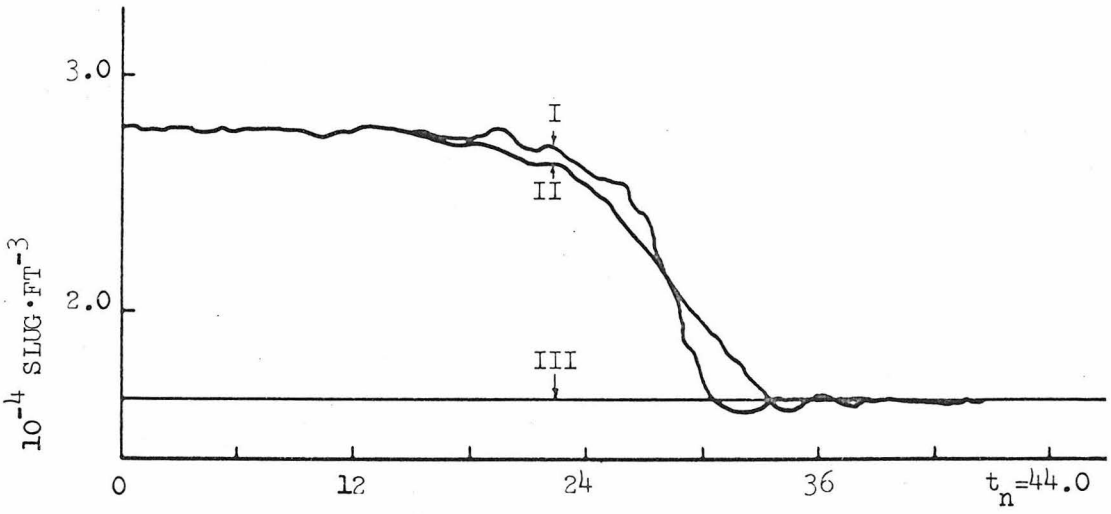

(b)

Figure 15. Parameter estimation of atmospheric density. Output of I = complete filter, II = approximate filter; III = true value: (a) Actually VM-4 was used but it was thought to be VM-10. (b) Actually VM-8 was used but it was thought to be VM-4.

how the state x_4 can be estimated when the Eqs. (4.22) and (4.23) are employed.

The sequential estimator under consideration requires the solution of as many as 14 nonlinear differential equations simultaneously. It is a natural consequence of this to investigate if further approximation of the filter is possible. Motivation of such an investigation is started from engineering considerations. In fact, simplification of the filter may be the most important consideration, as far as the implementation is concerned, for on line and real time calculations.

A simplification of the filter is suggested by making some of the elements of the matrix Γ to be constant, i.e.

$$\gamma_{ij}(t) = \gamma_{ij}(t_e + 10)$$

for $\forall\, t \in [t_{do}, t_n]$, where such (i, j) pairs are

$$(i,j) = (1,2),\ (1,3),\ (2,3)\ \&\ (2,4)$$

The resulting filter performance associated with the state x_4 is illustrated in Figure 15. It should be noticed that the filter performance is not degenerated by such simplification.

4.4 Discussions

4.4.1 A Quick Convergence Algorithm

The nonlinear filters under consideration are approximate ones. For this reason, goodness of the initial values of the unknown parameter becomes a prime importance. An algorithm is developed in order to obtain the unknown parameter systematically.

In the beginning of the atmospheric re-entry phase in which

the aerodynamic drag is negligible, the speed of the capsule is increasing due to the gravitational pull of the planet. As the capsule descends deep into the atmosphere, the braking effect of the atmosphere becomes significant. A full use is made of this phenomenon to derive a quick convergence algorithm of the unknown parameter. That is, zero detection of the acceleration yields a formula such as:

$$\mu_4 = \frac{2k_1 k_4 \sin \mu_2}{\mu_1} e^{k_5 \mu_3} \tag{4.26}$$

from Eq. (4.13). Hence, the quick convergence algorithm of the unknown parameter is given by the following:

(a) Start the sequential estimation given by Eq. (4.22) with the parameters of VM-4 atmospheric density model.

(b) If the estimated speed is increasing, continue the estimation with the current value of μ_4.

(c) If zero acceleration is detected, evaluate the new value for μ_4 according to Eq. (4.26).

(d) Repeat the sequential estimation with μ_4 obtained in (c) as the initial condition.

4.4.2 Conclusive Remarks

The closed form solutions denoted by Eqs. (3.37) and (3.38), and the successful parameter estimation through Eqs. (4.22) and (4.23) complete the trajectory design problem with partially known atmospheric environment. The success of such a design scheme is founded on the fact that the control force during the parameter estimation is independent of the possible atmospheric density. The quick convergence algorithm

of the unknown parameter is an immediate consequence of well behaved inertial observations.

The analytic trajectory design method discussed so far provides a way to a stochastic formulation of the problem, which is the next topic to be considered.

V. STOCHASTIC OPTIMAL CONTROL PROBLEM

5.1 Introduction

One of the most unique features of the investigation of this section is an introduction of random phenomena acting on the plant dynamics and on the observations. A great progress has been made in the formulation and solution of stochastic optimal control problems since the introduction of dynamic programming technique by Bellman.[47] Wonham[48] and Kushner[40,55] contributed to the pioneering work in the same field. However the solution of stochastic optimal control problems is difficult to obtain except for a restricted class of problems. The difficulties of the stochastic optimal control problem may be summarized as follows:

(a) There is very little known about the noise processes. In other words, there is no way to verify the justification of the particular mathematical noise model employed in the analysis.

(b) A rigorous interpretation+ of a differential equation with a white noise process in its forcing term has not been established yet.

In this particular problem, the main source of stochastic disturbances are wind and wind gust of the Martian atmosphere. Mathematical models of such stochastic disturbances are developed by utilizing Ornstein-Uhlenbeck processes.[50] The purpose of this investigation is to circumvent the random disturbances acting on the plant

---

+ For a class of such equations, Ito[42] and Stratonovich[39] gave some interpretations, which seem to be accepted[38] among mathematicians.

dynamics based upon noisy observations. It is suggested that a small thrust be utilized, for example a cold gas reaction jet, which is placed at an appropriate location of the capsule[18] for the attitude control purpose. It is required to minimize the expected value of the off target deviations with as small energy expenditures as possible. The feasibility of this formulation is shown using Monte Carlo simulations.[57] The investigation is then extended to the simplification of the optimal control law in order to facilitate a reasonable implementation of the resulting control law.

5.2 Martian Wind and Wind Gust Models

The flow of the Martian atmospheric gas has been observed in the last fifty years or so.[14] This has been done through the long term observations of the movement of the yellowish clouds[49] around Mars. It is reported[14,49] that the activities of the clouds, analogous to those of earth, are different at different locations and during seasons of Mars. In this investigation, no particular season or particular landing site has been assumed.

Two kinds of wind models are developed+, i.e. the surface wind model and the high altitude wind model. The surface wind model may be characterized as follows: If the wind speed at 300 ft above the local surface is $\bar{\omega}$, then the wind speeds are 0.8 $\bar{\omega}$ at the height of 30 ft, 0.07 $\bar{\omega}$ at 3 ft and zero at the surface. Wind directions are assumed to be parallel to the local terrain. On the other hand, the high

---

+ Data is referred to reference [18] etc.

altitude wind and wind gust models are assumed as follows: For elevations greater than 1,000 ft and less than 90.0×10^3 ft above the surface, the wind directions[+] are assumed normal and parallel to the local vertical. The maximum speeds for different atmospheric density models are given in Table 1. It is also assumed that the wind speed tails off at altitudes between 90.0×10^3 ft and $100. \times 10^3$ ft. No wind is assumed at altitude higher than $100. \times 10^3$ ft.

Mathematical models of the flow of atmospheric gas are developed. Let the speeds of horizontal and vertical flow of atmospheric gas be denoted by ς_x and ς_y, respectively. Then, it is a natural assumption that they satisfy the conditions such as:

$$E[\varsigma_x] = E[\varsigma_y] = 0 \tag{5.1}$$

where $E[\,\cdot\,] \triangleq$ an expectation operator. Similar to the atmospheric behaviour of the earth, the flows of the atmospheric gas of Mars can not change their directions abruptly, i.e. they have some inertia. This, in mathematical expression, can be described by:

$$\begin{aligned} E[\varsigma_x(t_1)\varsigma_x(t_2)] &= h_x(t_1 - t_2) \\ E[\varsigma_y(t_1)\varsigma_y(t_2)] &= h_y(t_1 - t_2) \end{aligned} \tag{5.2}$$

where $h_x(\,\cdot\,)$ and $h_y(\,\cdot\,)$ are even, monotone decreasing functions.

The stochastic process which satisfies both of these conditions,

---

[+] Only horizontal wind has been assumed in Voyager project documentation: Wind gust has been left unknown.

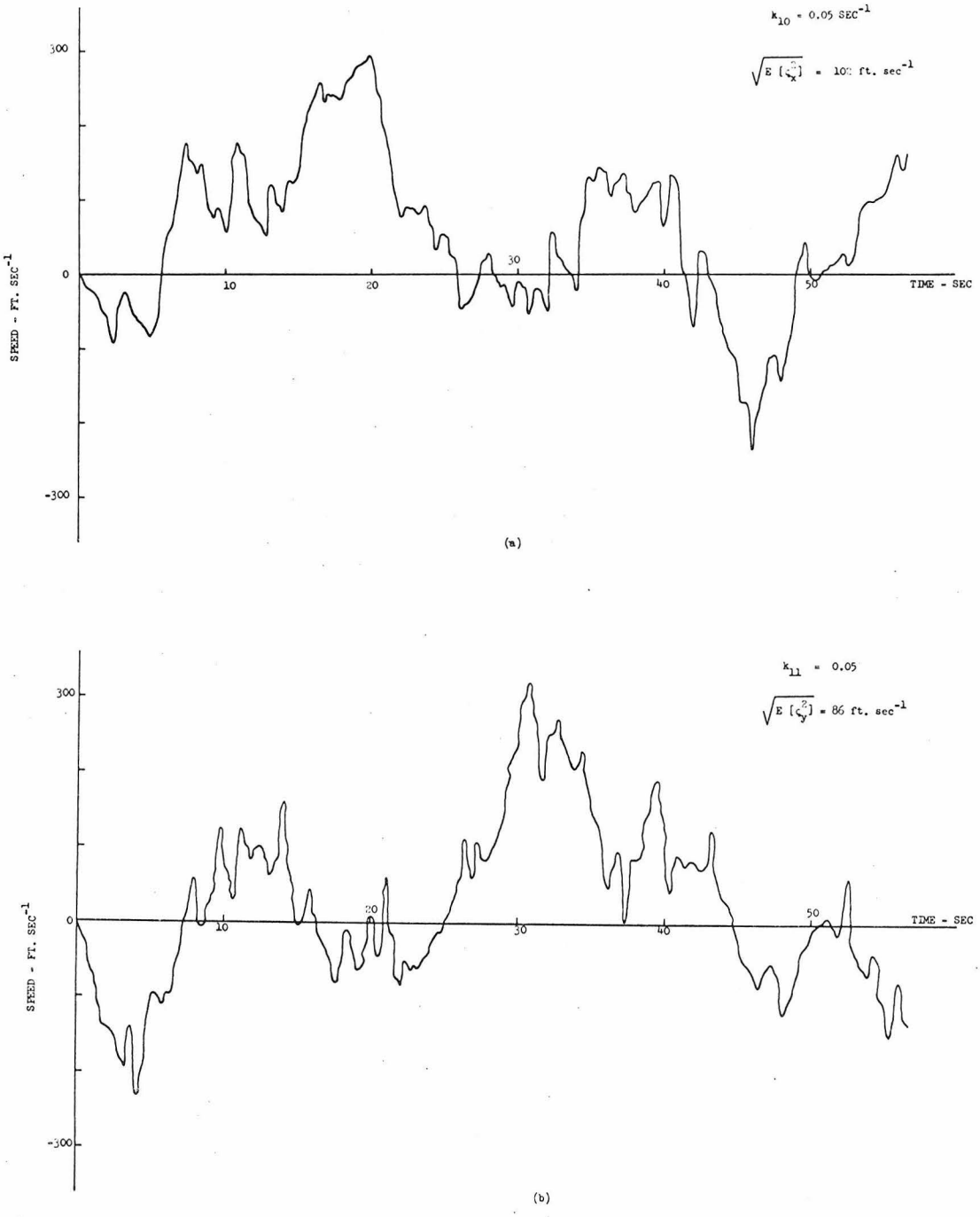

Figure 16. Typical wind and wind gust models:
(a) Horizontal; (b) vertical

and has mathematical tractability is the Ornstein-Uhlenbeck[+] process. That is, the Martian wind and wind gust models are characterized by:

$$d\varsigma_x = - k_{10} \varsigma_x \, dt + dw_x(t) \tag{5.3}$$

$$d\varsigma_y = - k_{11} \varsigma_y \, dt + dw_y(t) \tag{5.4}$$

where $\frac{dw_x}{dt}$ and $\frac{dw_y}{dt} \triangleq$ independent Gaussian white noise processes. The constants, k_{10}^{-1} and k_{11}^{-1}, characterize repetitive time constants of the O-U processes. Typical atmospheric behaviours of Mars generated by Eqs. (5.3) and (5.4) are illustrated in Figure 16.

5.3 Formulation of the Problem

5.3.1 Noisy Plant Dynamics

Since the stationarity condition of the Martian atmosphere is removed, reevaluation of the plant dynamics is necessary. It is observed from Figure 16, that the Martian wind and wind gust speed is much less than that of capsule throughout the atmospheric re-entry phase. Thus, neglecting the second order terms with respect to wind and wind gust, the noise corrupted dynamical system can be characterized by the following equations[++]:

[+] O-U process as abbreviated.

[++] It is assumed that the correlation time constants, k_{10}^{-1} and k_{11}^{-1}, are known. In actual situation, these parameters must be estimated. See Section 5.5.1 detailed discussions.

$$\frac{dx_1}{dt} = k_1 \sin x_2 - \frac{\rho(x_3)x_1^2}{2k_2} - \hat{x}_1 \frac{\rho(\hat{x}_3)}{k_2}(\cos \hat{x}_2)\, x_4 + \hat{x}_1 \frac{\rho(\hat{x}_3)}{k_2} (\sin \hat{x}_2)\, x_5 + v_1 \tag{5.5}$$

$$\frac{dx_2}{dt} = (\frac{k_1}{x_1} - \frac{x_1}{k_3}) \cos x_2 - \hat{u} \frac{\rho(x_3)}{2k_2} x_1 - \hat{u}\frac{\rho(\hat{x}_3)}{k_2} (\cos \hat{x}_2)\, x_4 - \hat{u} \frac{\rho(\hat{x}_3)}{k_2}(\sin \hat{x}_2)\, x_5 + \frac{v_2}{\hat{x}_1} \tag{5.6}$$

$$\frac{dx_3}{dt} = - x_1 \sin x_2 \tag{5.7}$$

$$dx_4 = - k_{10}x_4 dt + dw_x \tag{5.8}$$

$$dx_5 = - k_{11}x_5 dt + dw_y \tag{5.9}$$

It is assumed that the thrust, v_1 and v_2, can be controlled independently. No restriction is assumed on the magnitude of the thrust. The lift control $\hat{u}$ is determined by the switching boundaries such as:

$$\psi_1(\mu, k) = 0$$
$$\psi_2(\mu, k) = 0 \tag{5.10}$$

where $\mu \triangleq$ (an estimate of the vector x). For convenience, the system dynamics, i.e. Eqs. (5.5) through (5.9), are expressed in the following compact form:

$$dx = f(x, \hat{u}; k)\, dt + B(t)\, v\, dt + dw \tag{5.11}$$

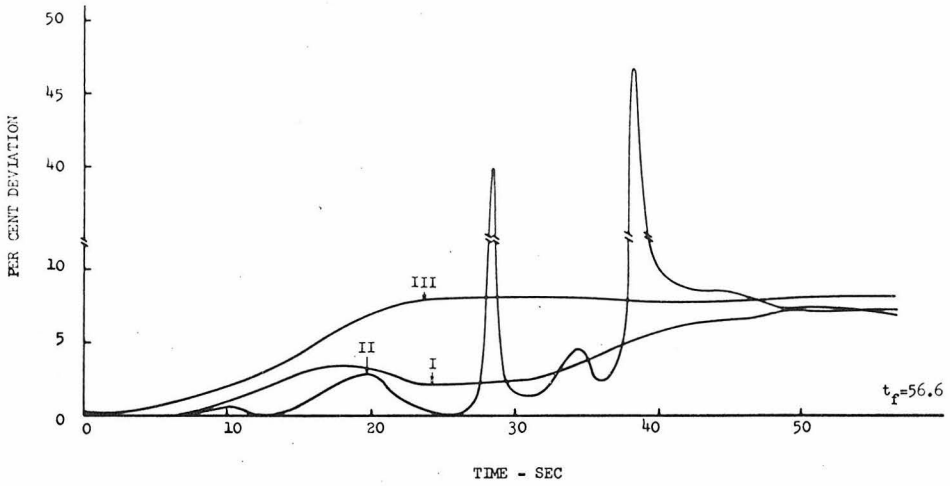

(Figure 17)

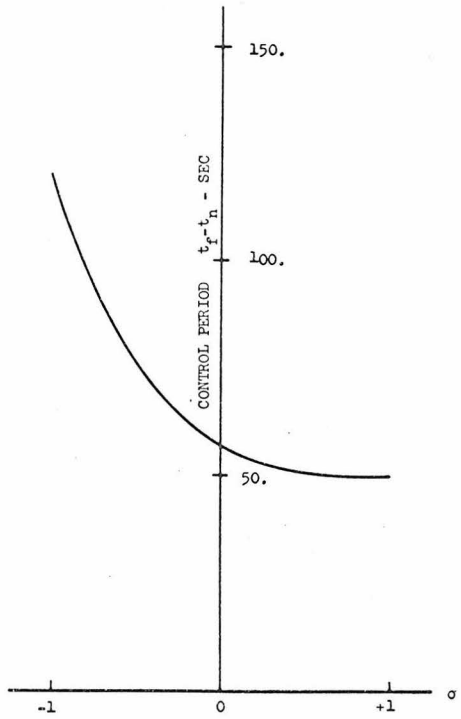

(Figure 18)

Figure 17. Off nominal trajectory deviation due to stochastic disturbances: I = velocity deviation; II = angular deviation; III = altitude deviation.

Figure 18. Decision of the terminal time.

where

$$B(t) \triangleq \begin{pmatrix} 1 & 0 & 0 \\ 0 & \hat{x}_1^{-1} & 0 \\ 0 & 0 & 0 \\ \hline & 0_{23} & \end{pmatrix} \tag{5.12}$$

$$dw \triangleq \text{col}\ (0,\ 0,\ 0,\ dw_x,\ dw_y) \tag{5.13}$$

It is reasonable to simulate this system in order to know by how much the trajectory is subject to the stochastic disturbances. In such a simulation, the thrust is set to be null. Figure 17 illustrates the results of a numerical experiment for a sample function of a white noise process. Off nominal value of the flight path angle, when it is expressed in per centage, increases sharply whenever it flies horizontally.

5.3.2 Presentation of the Problem

In a fixed terminal state stochastic optimal control problem, in general, it is impossible[52] to reach the terminal manifold within a fixed time unless the noise model belongs to a restricted class and the control force becomes infinity. Therefore, in order to make the formulation of this control problem meaningful it is required to minimize the off target deviations with as small energy expenditures as possible. The necessary time interval for the capsule to arrive at the target region is predetermined through the deterministic minimum heat generation problem. Figure 18 shows the time interval, $t_f - t_n$, which is necessary to guide the capsule with minimum heat generation. For any Martian atmospheric density which the capsule may encounter, i.e. for any value of

$$|\sigma| \leq 1 \ , \tag{5.14}$$

the corresponding time interval can be interpolated from this chart.

The performance index to be minimized is selected to be:

$$J \triangleq E[\|x(t_f) - x^{(N)}(t_f)\|_R^2 + \int_{t_n}^{t_f} \|v\|_{S(\tau)}^2 \, d\tau] \tag{5.15}$$

where $x^{(N)}(t) \triangleq$ a nominal trajectory[+],

$S(t) \triangleq$ a positive definite matrix for $\forall\, t \in [t_n, t_f]$,

$$R \triangleq (r_{ij}) \text{ with} \tag{5.16}$$

$$r_{ij} = \begin{cases} r_{ij}(>0) & : \text{ if } i, j = 1,3 \\ 0 & : \text{otherwise} \end{cases}$$

The matrix R has some reciprocal relation[53,54] with the convariance matrix of off target deviations. The above performance index implies minimization of two conflicting interests, i.e. accuracy of the trajectory at the terminal point and the energy consumed during the process.

In this problem, the observable quantities are only the flight path data obtained inertially. The observation vector, denoted by y, is given by:

$$y = Hx + \eta \tag{5.17}$$

where

$$H \triangleq (I_{33} \,\vdots\, 0_{32})$$

It should be noticed that the atmospheric parameter associated with the surface density is known to the system prior to the flight of the capsule in this phase.

[+] Defined in Section 5.4.1.

5.4 Solution of the Problem

5.4.1 Nominal Trajectory and Linearized System

The stochastic optimal control problem presented in the previous section is constrained by a system of nonlinear differential equations. Formal solution of such a problem requires the solution of the Bellman equation[46] for the problem. This equation, however, has been solved only for a restricted class of problems. Here lies the motivation for linearizing the system equations. The validity of such an approach has been shown elsewhere.[65]

When the capsule is under the influence of stochastic disturbances the atmospheric density is completely identified. A nominal trajectory, denoted by $x^{(N)}(t)$, is defined as:

$$x^{(N)}(t) = \hat{x}(t) - \Delta x_f \tag{5.18}$$

for $t \in [t_n, t_f]$, where

$\Delta x_f \triangleq$ an irreducible off target deviation.

The plant dynamics are approximated, within the accuracy of $\underline{o}(\|\delta x\|^2)$, by:

$$d(\delta x) = \{A(t)\delta x + B(t)v\}dt + dw \tag{5.19}$$

where $$\delta x \triangleq x - x^{(N)} \tag{5.20}$$

$$A(t) \triangleq \left(\frac{\partial f_i}{\partial x_j}\right)_{x = x^{(N)}} . \tag{5.21}$$

The performance index is rewritten by using the second variation such as:

$$J = E[\|\delta x(t_f)\|_R^2 + \int_{t_n}^{t_f} \|v\|_S^2 \, d\tau] \tag{5.22}$$

The above problem is a linear stochastic optimal control problem, which may yield a meaningful solution.

5.4.2 Optimal Control Law[48]

The dynamical system (5.19) perturbed by additive Gaussian white noise processes is a Langevin equation. Its solution is a random function which is a Markov process.[38] The minimization of the performance index (5.22)is investigated where the exact value of the vector δx is assumed to be known for each instant of time.

Let the cost function, denoted by $V(\delta x, t)$ associated with this problem, be defined as:

$$V(\delta x, t) = \min_v E[\|\delta x\|_R^2 + \int_t^{t_f} \|v\|_{S(\tau)}^2 d\tau] \tag{5.23}$$

The principle of optimality and the Markovian nature of the process δx yield a stochastic Bellman equation such as:

$$-\frac{\partial V}{\partial t} = \min_v [\|v\|_S^2 + \langle \frac{\partial V}{\partial(\delta x)} , A\delta x + Bv \rangle + \frac{1}{2} (\frac{\partial^2 V}{\partial(\delta x)^2}) \odot \Lambda] \tag{5.24}$$

where $$\Lambda dt \triangleq E[\, dwdw^*] \tag{5.25}$$

The symbol $\odot$ defines an operation described below: For matrices A and B of the same dimension:

$$A \odot B \triangleq \sum_{i \in I} \sum_{j \in J} a_{ij}\, b_{ij} \quad .$$

Carrying out the minimization operation, Eq. (5.24) yields the optimal control law such as:

$$\hat{v} = -\frac{1}{2} S^{-1} B^* \frac{\partial V}{\partial(\delta x)} \tag{5.26}$$

together with a stochastic Bellman Hamilton Jocobi equation given by:

$$-\frac{\partial V}{\partial t} = \left\langle \frac{\partial V}{\partial(\delta x)} , A\delta x \right\rangle + \frac{1}{2} \left(\frac{\partial^2 V}{\partial(\delta x)^2}\right) \odot \Lambda$$

$$- \frac{1}{4} \left\| \frac{\partial V}{\partial(\delta x)} \right\|^2_{BS^{-1}B^*} \quad . \tag{5.27}$$

Eq. (5.27) has the following solution[+]:

$$V(\delta x,\ t) = \|\delta x\|^2_{F(t)} + g(t) \quad . \tag{5.28}$$

The time varying gain functions, F(t) and g(t), are the solution of the following ordinary differential equations:

$$-\frac{dF}{dt} = FA + A^*F - F(BS^{-1}B^*)F \tag{5.29}$$

$$-\frac{dg}{dt} = F \odot \Lambda \tag{5.30}$$

[+] Such solution is unique.[48]

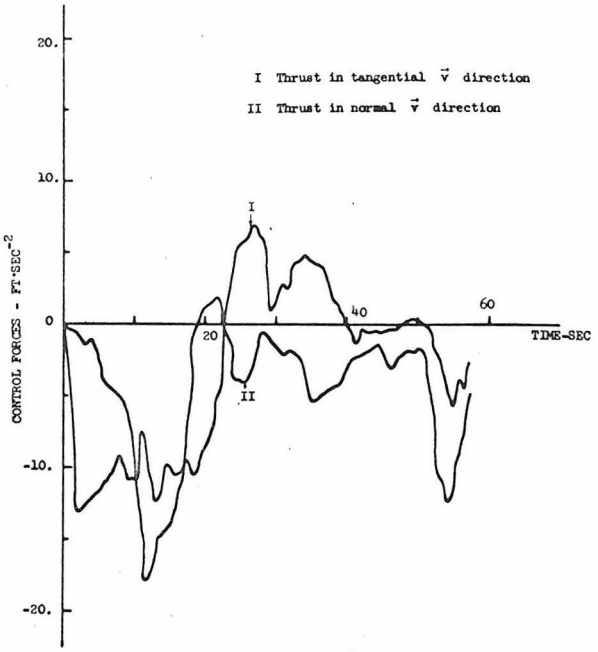

(a)

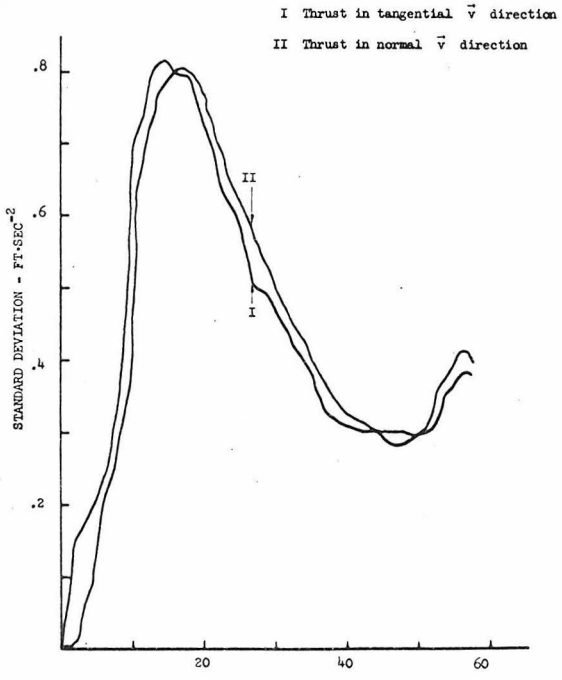

(b)

Figure 19. Control forces when the velocity is 5% off nominal at $t = t_n$: (a) Thrust vector; (b) standard deviation.

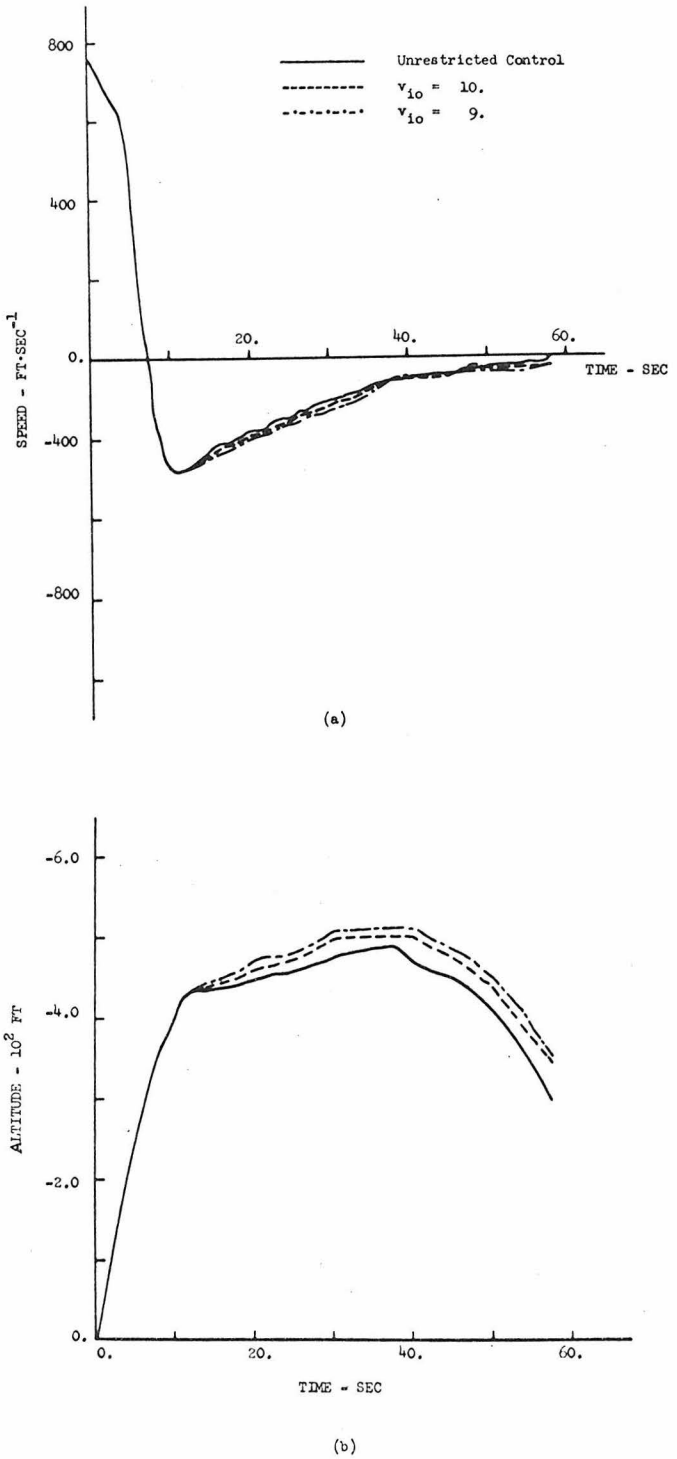

Figure 20. Controlled trajectory deviation when the velocity is 5% off nominal at $t = t_n$: (a) Speed deviations; (b) altitude deviations.

where the boundary conditions are given by:

$$F(t_f) = R \tag{5.31}$$

$$g(t_f) = R \circledcirc \Lambda \tag{5.32}$$

The optimal control law is, therefore, given by:

$$\hat{v}(t) = -S^{-1}B^* F\delta x \quad . \tag{5.33}$$

During the course of simulations, the feedback gain matrix $F(t)$ can be evaluated off line since Eq. (5.29) does not involve any term associated with the noise process or the random variable δx.

5.4.3 Monte Carlo Simulations

Several numerical experiments of the control law (5.33) are carried out using Monte Carlo simulations. Figure 19 depicts a typical pair of control thrusts, v_1 and v_2: Figure 20 illustrates the corresponding trajectory of δx.

Similar experiments are performed for the case in which the optimal control is limited from the above. That is, the control law (5.33) is chopped off if the value exceeds the given limit such as:

$$\hat{v}_i(t) = \begin{cases} \hat{v}_i(t) & ; \text{ if } |\hat{v}_i(t)| \leq v_{io} \\ v_{io} & ; \text{ otherwise} \end{cases} \tag{5.34}$$

where $i \in (1, 2)$. This is a Letov problem. It should be noticed that the resulting control law (5.34) is not optimal[56] anymore. Typical

Case I: 0% Deviation in Speed and Flight Path Angle

Sample Number	v_{io} = 00	v_{io} = 10. ft·sec^{-2}	v_{io} = 9.0 ft·sec^{-2}
1	.27064 x 10^4	.28747 x 10^4	.37592 x 10^4
2	.26784	.26784	.26784
3	.27298	.27293	.26893
4	.26787	.26787	.26787
5	.27084	.27084	.27083
6	.26827	.26827	.26827
7	.26996	.26996	.26996
8	.26817	.26817	.26817

Case II: 5% Deviation in Speed and Flight Path Angle

		Values of Performance Indices	
Sample Number	v_{io} = 00	v_{io} = 10.ft·sec^{-2}	v_{io} = 9.0 ft·sec^{-2}
1	.26908 x 10^4	.26903 x 10^4	.26899 x 10^4
2	.26800	.26794	.27518
3	.27300	.65570	1.07110
4	.27288	.26908	.28623
5	.27084	.27080	.27064
6	.26828	.37052	.47569
7	.27719	.27070	.37904
8	.26812	.30264	.33910

Table 3. Energy consumption for different sample functions of white noise processes: The values represent the quantity such as: $\int_{t_n}^{t_f} \|v\|_S^2 dt$

results are illustrated in Figure 20 for comparison.

By definition the linear optimal control law (5.33) is the optimal solution. However, what characterizes the peculiarity of a stochastic optimal control problem when compared with its deterministic counter part, is that the value of the performance index (5.22) is subject to change depending upon different sample functions of the stochastic processes involved. For this reason, Monte Carlo simulations are carried out in orther to investigate the necessary energy expenditures to accomplish the goal[+]. Table 3 shows the results of the simulations for different sample functions of the Gaussian white noise processes. Through these simulation results, the following conclusions are obtained:

(a) The necessary energy expenditures are almost indifferent if no limit is posed on the intensity of the thrust.

(b) The capsule may be blown away from the nominal trajectory, before it reaches the target, if a limited thrust is utilized.

Monte Carlo simulations are repeatedly carried out for different correlation times, k_{10}^{-1} and k_{11}^{-1}, of the stochastic processes. The results are summarized in Figure 21. From this figure, the following conclusions are obtained:

(a) A small energy expenditure is sufficient to guide the capsule to the target if the correlation times are small.

(b) On the other hand, a large energy is required to control the

---

[+] The maximum tolerance of off target deviations of speed and altitude are set to be 1 per cent and 3 per cent, respectively, of the nominal values.

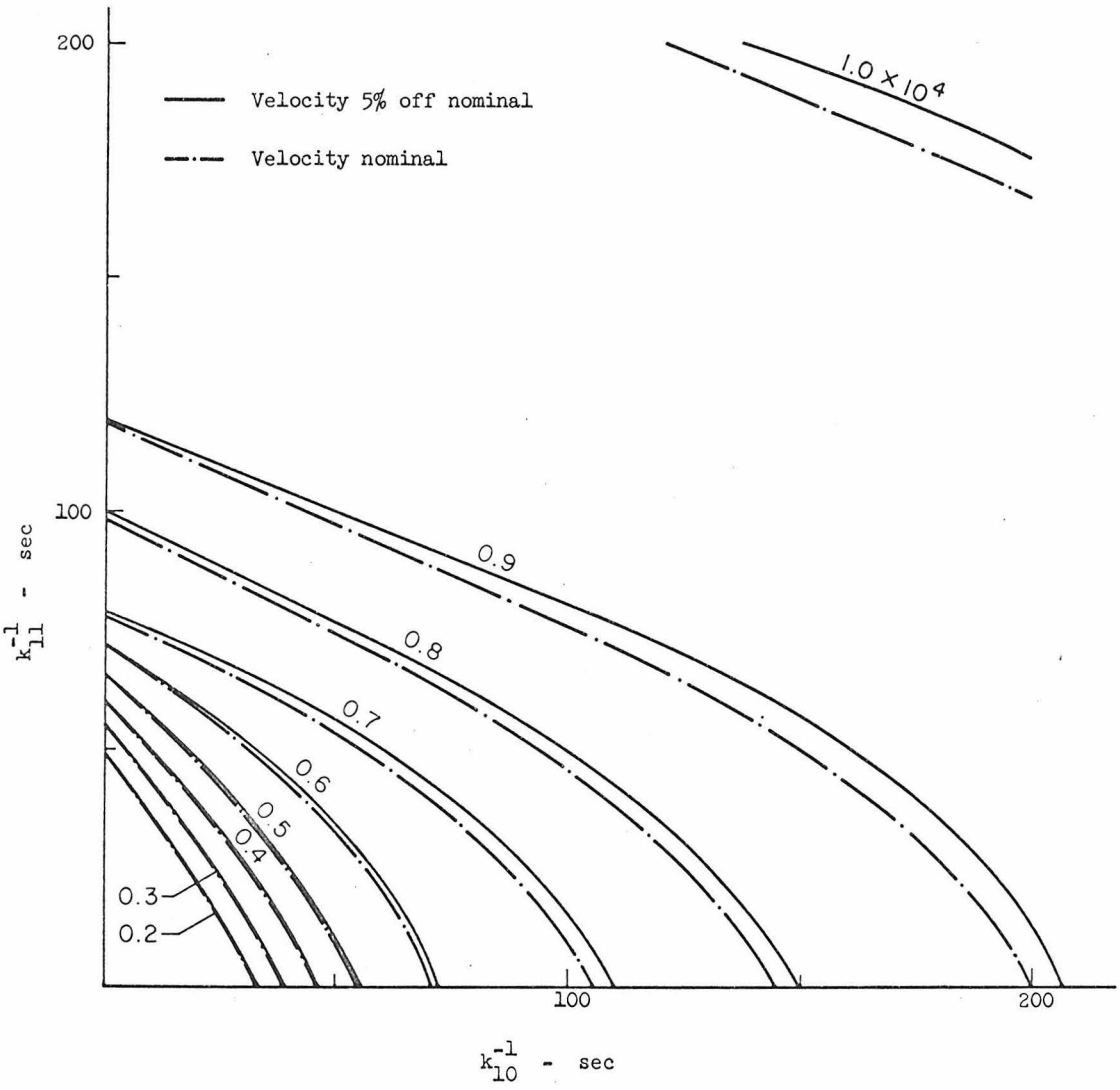

Figure 21. Equi-energy curves: The parameters represent the quantity such as:

$$\int_{t_n}^{t_f} \|v\|_S^2 \, dt$$

capsule which wanders away from the nominal trajectory due to wind and wind gust of the same directions throughout the flight time period $t_f - t_n$.

5.5 Suboptimal Control Law with State Estimation

5.5.1 General Discussions

The stochastic optimal control problem which is formulated and solved above is studied from an idealized standpoint. A drastic complication may be introduced in the actual situation, whenever:

(a) The correlation times, k_{10}^{-1} and k_{11}^{-1}, must be identified.

(b) The vector δx must be estimated at each instant of time.

The former requires an increase in the dimensionality of the plant equations. That is, Eqs. (5.8) and (5.9) must be replaced by:

$$dx_4 = - x_4 x_6 \, dt + dw_x \tag{5.35}$$

$$dx_5 = - x_5 \, x_7 \, dt + dw_y \tag{5.36}$$

$$\frac{dx_6}{dt} = 0. \tag{5.37}$$

$$\frac{dx_7}{dt} = 0. \tag{5.38}$$

The latter makes the situation even more difficult. That is, in order to estimate the instantaneous value of the vector such as

$$x = \text{col} \, (x_i : i \in (1, \ldots, 7)),$$

the only available data is

$$y_i = x_i + \eta_i : i \in (1, 2, 3) \quad . \tag{5.39}$$

A nonlinear filter for such a problem may result in numerical instability. Even though the estimation is performed successfully, the evaluation of the matrix Riccati equation (5.29) with a dimensionality of 7 by 7 would exceed the capability of an on board computer.

For these reasons, a modification of the stochastic optimal control law is investigated. Let the feedback gain matrix $F(t)$ be decomposed into sub matrices such as:

$$F(t) \triangleq \begin{pmatrix} F_{33}(t) & \vdots & F_{32}(t) \\ \cdots & \vdots & \cdots \\ F_{32}^*(t) & \vdots & F_{22}(t) \end{pmatrix} \tag{5.40}$$

Then, the following term associated with the control appears in the plant dynamics:

$$\mathcal{B} F\delta x = \begin{pmatrix} \mathcal{B}_{33}F_{33} & \vdots & \mathcal{B}_{33}F_{32} \\ \cdots & \vdots & \cdots \\ 0_{32}^* & \vdots & 0_{22} \end{pmatrix} \delta x \tag{5.41}$$

where

$$\mathcal{B} \triangleq \begin{pmatrix} \mathcal{B}_{33} & \vdots & 0_{32} \\ \cdots & \vdots & \cdots \\ 0_{32}^* & \vdots & 0_{22} \end{pmatrix} \triangleq BS^{-1}B^* \quad .$$

In Eq. (3.41), the term

$$\beta_{33} F_{32} \begin{pmatrix} \delta x_4 \\ \delta x_5 \end{pmatrix} \tag{5.42}$$

has little contribution to the control law as compared with the term

$$\beta_{33} F_{33} \begin{pmatrix} \delta x_1 \\ \delta x_2 \\ \delta x_3 \end{pmatrix}, \tag{5.43}$$

throughout the time interval $[t_n, t_f]$. This is an immediate consequence of the fact that the terminal condition of the sub-matrix F_{32} is given by

$$F_{32}(t_f) = 0_{32} \quad . \tag{5.44}$$

Thus, elimination of term (3.42) in Eq. (5.41) reduces the current problem into the following:

(a) Estimation of the vector

$x = \text{col}\,(x_i \; ; \; i \in (1, 2, 3))$

at each instant of time.

(b) Evaluation of the matrix Riccati equation such as:

$$-\frac{dF_{33}}{dt} = A_{33}^{*} F_{33} + F_{33} A_{33} - F_{33} \beta_{33} F_{33} \tag{5.45}$$

Further discussions of these problems appear in the following two sections.

5.5.2 Estimation of the State

The sequential estimation of the state variable $x(t)$ requires the solution of an integro-partial differential equation[40,46,55] associated with the nonlinear system given by Eqs. (5.5) through (5.9). Such an equation has not been solved except for a restricted class of problems. Thus, a reasonable approximate scheme must be introduced. A Kalman filter which is applied to a linearized equation of a nonlinear system may give rise to an unacceptable filter performance.[37,41] An approximate filter shall be investigated to circumvent this difficulty.

So far, as many as seven different approximate nonlinear filters[36] are reported in the literature. The filtering scheme proposed by Detchmendy and Sridhar[44] will be used for this problem, since this filter does not require any statistical assumptions on the stochastic disturbances acting on the plant as well as on the observation.

A sequential estimator similar to that discussed in Section 4.3.2, but without parameter estimation, is derived. That is, the best estimate

$$\nu = \mathrm{col}(\nu_i:\ i\epsilon(1,2,3)) ,$$

in the similar sense as Eq. (4.20), is given by the solution of the following differential equations+:

$$\frac{d\nu}{dt} = f(\nu,\ \hat{u};\ k) + 2\ \Delta Q(y - \nu) \tag{5.47}$$

+ $\overline{P} \triangleq 3 \times 3$ submatrix in upper left corner of the matrix A.

$$\frac{d\Delta}{dt} = \frac{\overline{P}}{2} + \Delta \left(\frac{\partial f}{\partial x}\right)^{*}_{x=\nu} + \left(\frac{\partial f}{\partial x}\right)_{x=\nu} \Delta - \Delta Q \Delta \tag{5.48}$$

with

$$\nu_i(t_n) = \mu_i(t_n) \qquad i \epsilon (1,2,3)$$

$$\Delta\ (t_n) = \overline{P}_o$$

It is not a difficult task to obtain a good estimate from Eqs. (5.47) and (5.48) since the linear observations given by Eq. (5.39) already represent approximately the true value. Thus, the effort is concentrated in simplification of the filter. This is accomplished simply by letting[+]

$$\Delta\ (t) \equiv \begin{pmatrix} 10 & 0 & 0 \\ 0 & 1. & 0 \\ 0 & 0 & 0.1 \end{pmatrix} \tag{5.49}$$

for $\forall\ t \epsilon [t_n,\ t_f]$.

In order to denomstrate the validity of such simplification numerical experiments are carried out. Figure 22 shows the performance of the simplified filter for the most critical observational condition. That is, the observational noise is assumed to be of the form[++]

$$\eta_i(t) = (\text{Max}\ |\eta_i(t)|)\ \theta \tag{5.50}$$

[+] By same reasoning as discussed in 3.4.

[++] Two spikes in $\eta_2(t)$ are smoothed.

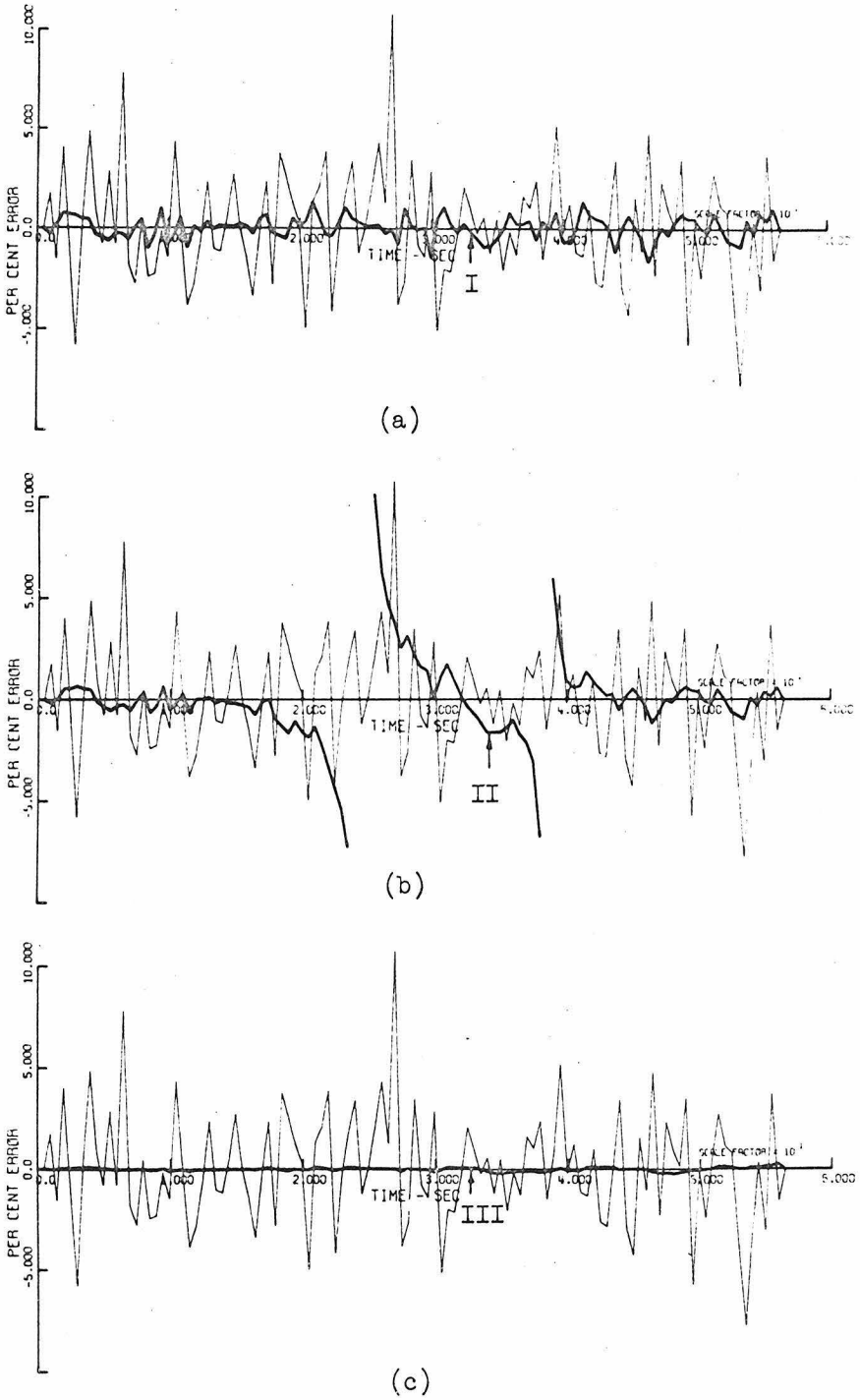

Figure 22. Performance of nonlinear filter. Scale factor of vertical axes is 10^{-1}. I = error in estimation; II = error in observation: (a) Speed; (b) flight path angle; (c) altitude.

where θ = Normal (0,1). It is seen from this result that a simplified filter may accomplish estimation of flight path data within acceptable accuracy.

5.5.3 Suboptimal Stochastic Control Law

Numerical integration of the matrix Riccati equation (5.45) gives rise to a difficult problem. That is, there is a direction in which Eq. (5.45) is numerically unstable. For the particular matrix denoted by:

$$A_{33}(t) = \left(\frac{\partial f_i}{\partial x_j}\right)_{x=x(N)}; \; i, \; j \in (1,2,3)$$

forward integration of Eq. (5.45) falls into this category. Since some elements of $A_{33}(t)$ are functions of the atmospheric density ρ and its parameters, it is not feasible to calculate Eq. (5.45) off line[+] and store the data in some memory media. This is the motivation for the following approximation.

It is observed that the matrices $A_{33}(t)$ and $\mathcal{B}_{33}(t)$ have slowly time varying elements. Thus, matrices A_{33} and $\mathcal{B}_{33}$ may be approximated by constant matrices such as:

$$A_{33}(t) \cong \bar{A}_{33} \tag{5.51}$$

$$\mathcal{B}_{33}(t) \cong \bar{\mathcal{B}}_{33} \tag{5.52}$$

[+] Before the mission.

Substitution of Eqs. (5.51) and (5.52) into Eq. (5.45) results in a matrix Riccati equation with time invariant coefficients such as:

$$-\frac{d\bar{F}_{33}}{dt} = \bar{A}^{*}_{33}\,\bar{F}_{33} + \bar{F}_{33}\,\bar{A}_{33} - \bar{F}_{33}\,\bar{B}_{33}\,\bar{F}_{33} \tag{5.53}$$

with $$\bar{F}_{33}(t_f) = R \quad . \tag{5.54}$$

A matrix Riccati equation with constant coefficients can be solved[43] analytically.

Let the constant matrices be given by+

$$\bar{A}_{33} \triangleq \begin{pmatrix} -0.1116 & 0.1136 \times 10^{2} & 0.1205 \times 10^{-1} \\ 0. & -0.1718 \times 10^{-2} & 0. \\ -0.2579 & -0.1402 \times 10^{+4} & 0. \end{pmatrix} \tag{5.55}$$

$$\bar{B}_{33} \triangleq \begin{pmatrix} 1. & 0. & 0. \\ 0. & 10^{-8} & 0. \\ 0. & 0. & 0. \end{pmatrix} \tag{5.56}$$

Let a matrix $X(\tau)$ be defined as

$$X(\tau) = \begin{pmatrix} X^{(11)}(\tau) & 0_{33} \\ X^{(12)}(\tau) & X^{(22)}(\tau) \end{pmatrix}$$

which is the solution of an auxiliary differential equation given by:

$$\frac{dX}{d\tau} = \begin{pmatrix} \bar{A}^{*}_{33} & 0_{33} \\ \bar{B}_{33} & -\bar{A}_{33} \end{pmatrix} X(\tau) \tag{5.57}$$

+ Average value of each element.

with $X(o) = I_{66}$

$$\tau \triangleq t_f - t \ .$$

Then, Eq. (5.53) has a solution such as:

$$\bar{F}_{33}(t) = X^{(11)}(t)\ R\ \{X^{(12)}(t)\ R + X^{(22)}(t)\}^{-1}$$

$$= \{\mathbb{P} + \mathbb{Q}_2(t)(R - P)\mathbb{Q}_1^{-1}(t)\}^{-1} \qquad (5.58)$$

where $$\mathbb{P} \triangleq (\bar{A}_{33} + \Lambda)^{-1}\, \mathbb{B}_{33} \qquad (5.59)$$

$$\mathbb{Q}_1(t) \triangleq C\, e^{\Lambda(t_f - t)}\, C^{-1} \qquad (5.60)$$

$$\mathbb{Q}_2(t) \triangleq D\, e^{-\Lambda(t_f - t)}\, D^{-1} \qquad (5.61)$$

Matrices Λ, C and D are defined as follows:

$$\Lambda \triangleq \begin{pmatrix} -0.1718 \times 10^{-2} & 0. & 0. \\ 0. & -0.5336 \times 10^{-1} & 0. \\ 0. & 0. & -0.5824 \times 10^{-1} \end{pmatrix}$$

where the diagonal elements are the eigenvalues of the matrix $\bar{A}_{33}$.

$$C \triangleq \begin{pmatrix} 0. & 0. & 1. \\ 1. & 0.5631 \times 10^{4} & 0.5649 \times 10^{4} \\ 0. & -0.2258 & -0.2069 \end{pmatrix}$$

$$D \triangleq \begin{pmatrix} -0.5794 & 1. & 1. \\ 1. & 0. & 0. \\ -0.5378 \times 10^{5} & 4.833 & 4.428 \end{pmatrix}$$

where the column vectors $\underline{c}^{(i)}$ and $\underline{d}^{(i)}$ are the i - th eigenvectors of matrices $\bar{A}_{33}^{*}$ and $-\bar{A}_{33}$, respectively.

Suboptimal control law $\hat{\hat{v}}$ with state estimation is given by:

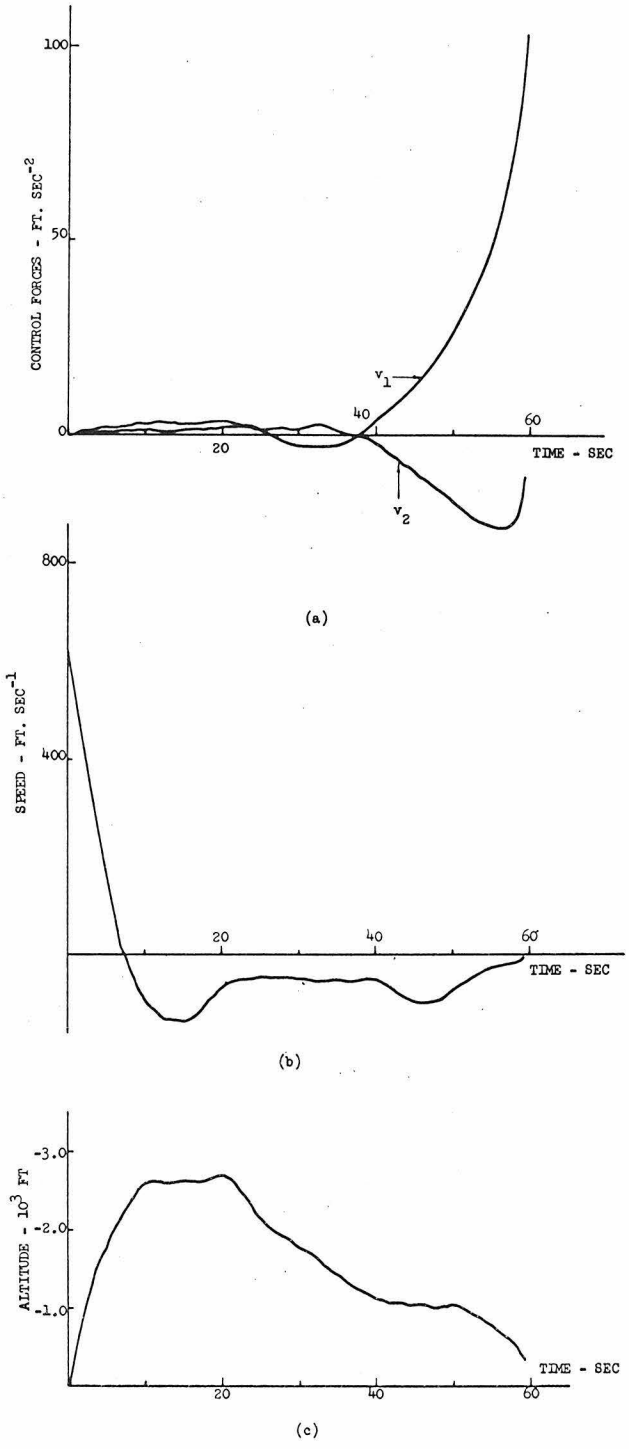

Figure 23. Control forces of the simplified controller; the velocity deviation at $t = t_n$ is 5%: (a) Thrust vector; (b) speed deviations; (c) altitude deviations.

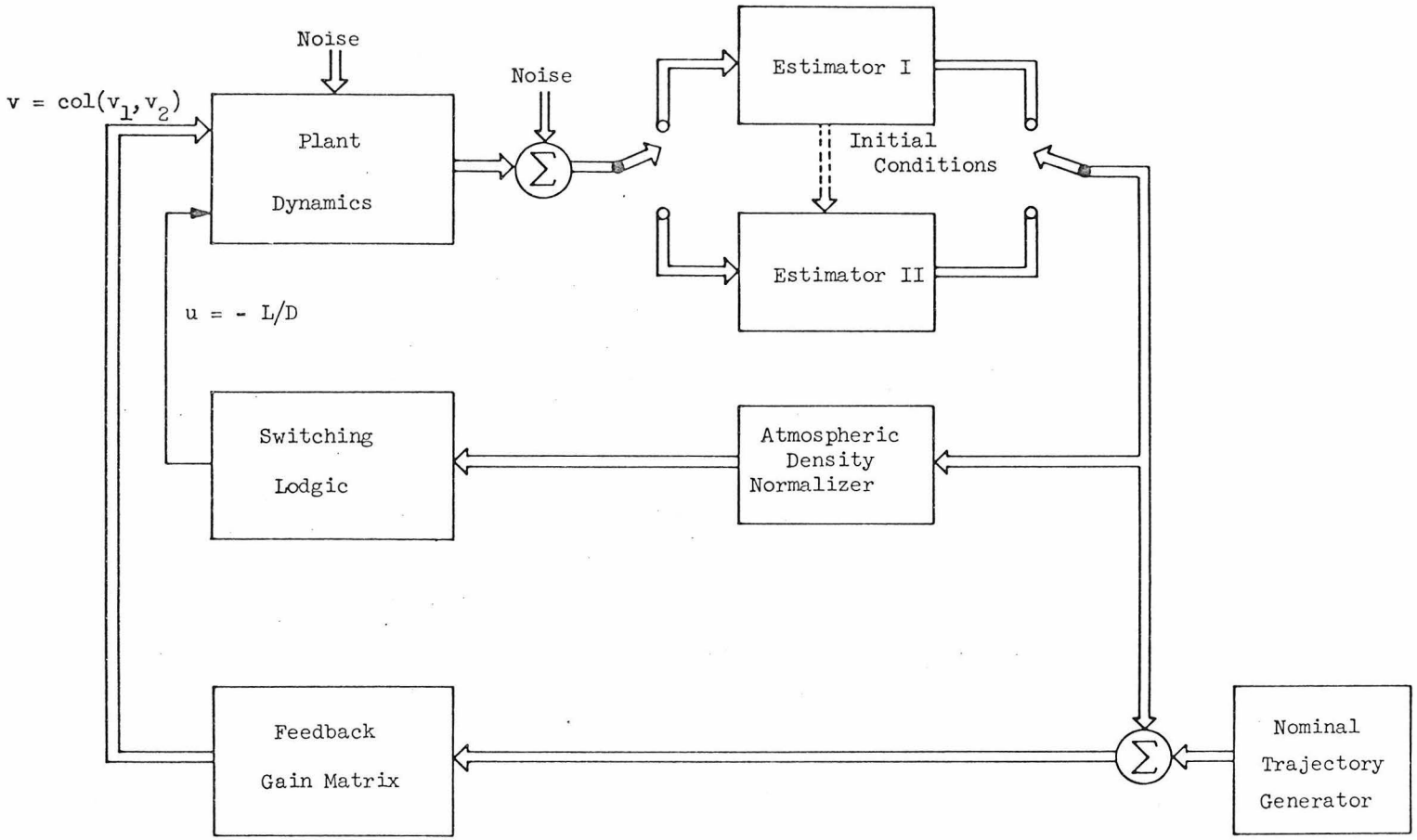

Figure 24. Composite re-entry control and guidance system: Estimator I is switched to Estimator II when the capsule arrives at the altitude of 100. x 10^3 ft.

$$\hat{\hat{v}}(t) = -S^{-1}B^{*}\overline{F}_{33}(t)\ (\mu - x^{(N)}) \qquad (5.62)$$

Figure 23 illustrates a typical thrust program, and the corresponding off nominal trajectory of the capsule.

Significant innovations of this approach are:

(a) Feedback gain matrix $\overline{F}_{33}(t)$ is given analytically.

(b) The load of on board computer is reduced drastically.

(c) The suboptimal control (5.62) does not degrade the necessary accuracy at the target. For the case when $k_{10} = k_{11} = 0.05$, the suboptimal control scheme uses about 1.4 times more energy than the optimal control scheme.

A complete feedback control system with suboptimal stochastic adjusting capabilities is illustrated in Figure 24.

5.6 Discussions

5.6.1 Conclusive Remarks

Feasibility of the stochastic optimal feedback control law has been demonstrated through repeated applications of Monte Carlo simulations. A simplification of the control law has also been accomplished. However, the engineering aspect of the problem, i.e. mechanization of the means of obtaining the desired thrust vectors, $\hat{v}_1$ and $\hat{v}_2$, with sufficient accuracy still remains unsolved.

Utilization of a finer control, such as variable lift to drag ratio, seems almost unsolvable for the associated minimum variance type control problem.

VI CONCLUSION

6.1 Introduction

The main purpose of this investigation is to demonstrate a feasibility of application of modern control theory to a class of engineering problems. There are two basic motivations for engineers to optimize the solution of a given practical problem. The first one is to check the goodness of a solution obtained by conventional trial and error approaches: The second one is that no solution other than the optimal one may possibly be accepted due to economical and/or physical reasons. An open loop solution may suffice the former motivation. On the other hand, the latter requires a feedback control law which automatically controls the system behaviour according to the desired requirement. The purpose of this investigation clearly falls into the second category.

6.2 Conclusive Remark

Feasibility of a gliding type re-entry of a space capsule into the Martian atmosphere has been investigated. An approximate control law was obtained in closed form for the problem of re-entry of a space capsule into a partially known atmosphere of Mars. Numerical simulations verified that such a control law which utilizes neighbouring trajectories compares favorably with the open loop control which minimizes the heat generation of the re-entry capsule. It was also shown that the minimum heat generation trajectory is identical with the minimum time trajectory. However, questions of controlability and uniqueness of the optimal control associated with such a re-entry scheme were beyond

the scope of the investigation.

A nonlinear filter which enables a sequential estimation of the states of the re-entry dynamics as well as the unknown parameters was constructed. A simplification of such a filter was achieved without degrading the resulting filter performance.

The guidance problem of a re-entry capsule under stochastic disturbances was also studied. Reasonable wind and wind gust models of Martian atmosphere were constructed in mathematical terms. Feasibility of guidance of the capsule with the minimum energy expenditures, when the capsule is in a stochastic disturbance environment, has been verified by Monte Carlo simulations.

The present investigation was concerned with a re-entry trajectory of a capsule for a wide range of plausible atmospheric density models of Mars. A drastic improvement of the investigation can be achieved when the Mariners VI and VII, both of which are traveling towards Mars, bring more precise scientific information about the Martian atmosphere in August 1969.

APPENDIX A

NOMENCLATURE

A_o	=	reference area of capsule, ft^2
C_D, C_L	=	aerodynamic drag and lift coefficient
d	=	aerodynamic drag due to wind and wind gust, lb
D	=	aerodynamic drag, lb
G	=	universal gravitational constant, ft^3/sec^2. slug
h_f	=	target altitude, ft
k_1	=	gravitational constant of Mars, ft/sec^2
k_2	=	ballistic constant, $slug/ft^2$
k_3	=	radius of Mars, ft
k_4	=	surface density parameter in stratosphere, $slug/ft^3$
k_5	=	inverse scale height in stratosphere, 1/ft
k_6	=	surface density parameter in troposphere, $slug/ft^3$
k_7	=	inverse scale height in troposphere, 1/ft
k_8	=	lowest attainable altitude, ft.
k_9	=	convective heat constant
k_{10}, k_{11}	=	inverse correlation time constant, 1/sec
k_{12}	=	tropopause altitude, ft
k_{13}	=	constant ($=G M_m$), ft^3/sec^2
L	=	aerodynamic lift, lb
ℓ	=	aerodynamic lift due to wind and wind gust, lb
m	=	mass of capsule, slug
M	=	mol weight of Martian atmosphere
M_m	=	mass of Mars, slug
P_o	=	atmospheric pressure on Martian surface, mb

q_c = convective heat transfer rate, BTU/$ft^{3/2}$.sec

r_{do} = distance from the centre of Mars at deorbit, ft

r_{pb} = periapsis distance of fly-by bus, ft

r_∞ = distance from the centre of Mars at separation, ft

R = ideal gas constant

R_n = nose radius of capsule, ft

t_b = time at skip up, sec

t_{do} = time at deorbit of capsule, sec

t_c = time at atmospheric re-entry, sec

t_f = time at target, sec

t_{s1} = time at the first switching boundary, sec

t_{s2} = time at the second switching boundary, sec

t_∞ = time at bus and capsule separation, sec

T_n = torque in normal direction of x_1

T_o = surface temperature, ^oK

T_p = period of circular orbit of capsule, sec

T_t = torque in tangential direction of x_1

x_1 = speed of capsule, ft/sec

x_2 = flight path angle, radian

x_3 = altitude, ft

x_4 = unknown parameter$^+$, constant

x_4 = wind and wind gust^{++}, in horizonal direction, ft/sec

x_5 = wind and wind gust, in vertical direction, ft/sec

$^+$ In Chapter IV

$^{++}$ In Chapter V

u = lift to drag ratio control

u_o = maximum value of lift to drag ratio control

γ_c = the largest re-entry angle, radian

γ_s = the smallest re-entry angle, radian

Γ = adiobatic lapse rate, $^oK/K_m$

η = observational noise vector

λ = Lagrange multiplier

ρ = atmospheric density of Mars, $slug/ft^3$

σ = normalized atmospheric density of Mars

ψ_i = i-th switching boundary

The following notation denotes the inner product of two n-dimensional vectors a and b:

$$\langle a, b \rangle \triangleq \sum_{i=1}^{n} a_i b_i \quad .$$

I_{mm} denotes an m by m identity matrix such as:

$$I_{mm} \triangleq \begin{pmatrix} 1 & 0 & 0 & \dots & 0 \\ 0 & 1 & 0 & \dots & 0 \\ 0 & 0 & 1 & \dots & 0 \\ \dots & \dots & \dots & \dots & \dots \\ 0 & 0 & 0 & \dots & 1 \end{pmatrix} .$$

0_{nm} denotes an n by m matrix with zero elements such as:

$$0_{nm} \triangleq \begin{pmatrix} 0 & \dots & 0 \\ \vdots & & \vdots \\ 0 & \dots & 0 \end{pmatrix} .$$

$*$ denotes a transpose of a matrix such as:

$$A^* = (a_{ij})^* = (a_{ji})$$

APPENDIX B

DECISION OF SWITCHING BOUNDARIES

The first switching boundary is defined as a family of trajectories which satisfy the boundary condition:

$$\begin{aligned} x_1(t_{s1}) &= \text{unspecified} \\ x_2(t_{s1}) &= 0 \\ x_3(t_{s1}) &= h_b \quad . \end{aligned} \tag{B.1}$$

In the neighbourhood of the skip-up point of the trajectory, terms due to the gravitational field and the centrifugal force are negligible compared with those due to aerodynamic forces. Thus, the system dynamics can be approximated by:

$$\frac{dx_1}{dt} \cong - \frac{\rho(x_3)\, x_1^2}{2k_2} \tag{B.2}$$

$$\frac{dx_2}{dt} \cong - \frac{\rho(x_3)\, x_1}{2k_2}\, u \tag{B.3}$$

$$\frac{dx_3}{dt} = - x_1 \sin x_2 \tag{B.4}$$

Skip-up phenomenon immediately implies that the control is

$$u(t) = + u_o = + L/D. \tag{B.5}$$

Time independent solution of the system, i.e. Eqs. (B.2) through (B.4), with conditions, i.e. Eqs. (B.1) and (B.5), is given by:

$$\cos x_2 = \begin{cases} 1 + \dfrac{u_o}{2k_2k_7}\{\rho(x_3) - \rho(k_8)\} : \text{if } x_3 \le k_{12} \\ \\ 1 + \dfrac{u_o}{2k_2}\left\{\dfrac{\rho(k_{12}) - \rho(k_8)}{k_5} + \dfrac{\rho(x_3) - \rho(k_{12})}{k_7}\right\} : \text{if } x_3 > k_{12} \end{cases} \tag{B.6}$$

Similarly, the second switching boundary is a family of trajectories which satisfy the terminal conditions:

$$x_1(t_f) = V_f$$

$$x_2(t_f) = \text{unspecified} \tag{B.7}$$

$$x_3(t_f) = h_f$$

The process of solving the dynamical equations:

$$\frac{dx_1}{dt} = k_1 \sin x_2 - \frac{\rho(x_3)x_1^2}{2k_2} \tag{B.8}$$

$$\frac{dx_2}{dt} = \left(\frac{k_1}{x_1} - \frac{x_1}{k_3}\right)\cos x_2 - u\,\frac{\rho(x_3)x_1}{2k_2} \tag{B.9}$$

$$\frac{dx_3}{dt} = -x_1 \sin x_2 \tag{B.10}$$

require the use of the second order theorem of planetary re-entry mechanism. Eqs. (B.8) through (B.10) can be rewritten in time independent form:

$$\frac{d}{d\rho}\cdot\left(\frac{x_1^2}{k_1k_3}\right) + \frac{1}{k_3k_7}\,\frac{\cos x_2}{\rho(x_3)}\left(\frac{k_1k_3}{x_1^2} - 1\right) = \frac{u}{2}\,\frac{1}{k_2k_7} \tag{B.11}$$

$$\frac{d}{d\rho} \cdot \left(\frac{x_1^2}{k_1 k_3}\right) + \frac{1}{k_2 k_7 \sin x_2} \left(\frac{x_1^2}{k_1 k_3}\right) = \frac{2}{k_3 k_7} \cdot \frac{1}{\rho(x_3)} \qquad \text{(B.12)}$$

In order for the capsule to reach the target altitude with the minimum time, the control must be

$$u(t) = - u_o = - L/D. \qquad \text{(B.13)}$$

By observing that the particular grouping of variables such as:

$$\frac{1}{k_2 k_7} \cdot \frac{\cos x_2}{\rho(x_3)} \cdot \left(\frac{k_1 k_3}{x_1^2} - 1\right)$$

is relatively insensitive to the integration over ρ and x_2, Eq. (B.11) can be integrated out to yield:

$$\cos x_2 = \cos x_2(t_f) + Z \{ \rho(x_3) - \rho(h_f)\} \qquad \text{(B.14)}$$

where

$$Z \triangleq - \frac{u_o}{2} \cdot \frac{1}{k_2 k_7} - \frac{\cos x_2}{k_2 k_7 \rho(x_3)} \cdot \left(\frac{k_1 k_3}{x_1^2} - 1\right) . \qquad \text{(B.15)}$$

Similarly, Eq. (B.12) can be integrated under the same condition to yield:

$$x_2 - x_2(t_f) = Z k_2 k_7 \ln \left(\frac{x_1}{v_f}\right)^2 \qquad \text{(B.16)}$$

Elimination of the unknown parameter $x_2(t_f)$ from Eqs. (B.14) and (B.16) yields the second switching boundary:

$$\cos x_2 = \cos \{x_2 + k_2 k_7 Z \ln \left(\frac{v_f}{x_1}\right)^2\} + \frac{Z}{2} \{ \rho(x_3) - \rho(h_f)\} \qquad \text{(B.17)}$$

LIST OF REFERENCES

[1] Chapman, D. R., "An Approximate Analytical Method for Studying Entry into Planetary Atmospheres," Tech. Rpt. R-11, Ames Research Center, Moffett Field, Calif.

[2] Bryson, A. E., et al., "Determination of Lift or Drag Programs to Minimize Re-entry Heating," J. of the Aerospace Sciences, April 1962.

[3] Dobrzanski, J. S., "Effect of Trajectory Control Scheme on the Performance of Lift Entry Vehicles," J. Spacecraft, Vol. 4, No. 2, February 1967.

[4] Leondes, C. T., and Nieman, R. A., "Optimization of Aerospace Re-Entry Vehicle Trajectories through Independent Control of Lift and Drag," J. Spacecraft, Vol. 3, No. 2, May 1966.

[5] Eggers, A. J., et al., "A Comparative Analysis of the Performance of Long-Range Hypervelocity Vehicles," Tech. Note, NACA TN 4046, 1958.

[6] Loh, W. H. T., "A Second-Order Theory of Entry Mechanics into a Planetary Atmosphere," J. of Aerospace Sciences, October 1962.

[7] Citron, S. J., and Meir, T. C., "An Analytic Solution for Entry into Planetary Atmospheres," AIAA, Vol. 3, No. 3, March 1965.

[8] Moore, J. W., "An Error Analysis of a 'Limited' Retro Lander System," JPL TM 343-78, Pasadena, Calif., June 1968.

[9] McMullen, J. C., and Smith, A. M., "Martian Entry Capsule: Design Considerations for Terminal Deceleration," Symposium of Dynamics of Manned Lifting Planetary Entry, John Wiley and Sons Co., 1963.

[10] Pritchard, E. B., and Harrison, E. F., "Analysis of Mars Entry with Consideration of Separation and Line-of-Sight Relay Communication for Bus-Capsule Combination," NASA TND-2841, May 1965.

[11] Cefola, P. J., "Adaptive Trajectory Control," NASA Grant NGR 33-018-091, Rensselaer Polytechnic Institute, Troy, New York, May 1968.

[12] Nieman, R. A., "Use of Variable Lift Control to Optimize Aerodynamic Braking for a Mars Entry Vehicle," Report No. 67-34, July 1967, Dept. of Engineering, UCLA.

[13] Mankowitz, R. J., "The Analysis and Configuration of a Control System for a Mars Propulsion Lander," JPL Technical Report, No. 32-1104.

[14] "Mars Atmosphere Definition: Final Report: Voyager Spacecraft," NASA CR-61185, January 1968.

[15] Sridhar, R., "Quarterly Report to JPL," JPL Contract No. 69821-69822, Jet Propulsion Lab., Pasadena, Calif.

[16] Ohtakay, H., "The Optimal Gliding Re-entry into Martian Atmosphere," JPL Tech. Memo-343-106, Jet Propulsion Lab., Pasadena, Calif.

[17] Kopf, E. H., "A 'Building Block' Simulation of a Mars Atmosphere Probe," JPL Inter-Office Memo, January 1968.

[18] "1973 Voyager Capsule Systems Constraints and Requirements Documents," JPL File SE3BC-6K-009.

[19] Jensen, J., Kraft, J. D., and Townsend, G. E., "Orbit Mechanics. Orbit Flight Handbook Part I -- Basic Technique and Data," NASA TND-1316, 1962.

[20] Barber, T. A., "Voyager Satellite Orbit Determination Accuracy Using Earth-Based Doppler Radar -- Part I -- Classical Orbital Element and Position Accuracies," JPL TM312-306, May 1963.

[21] Virzi, R. A., "Satellite Orbit Determination Accuracy Using On-Board Instruments," JPL TM 343-37.

[22] Teitis, P. H., "Translational and Rotational Motion of a Body Entering Mars Atmosphere," JPL Tech. Rpt. TR No. 32-845.

[23] Demile, F. A., "A Study of the Convective and Radiative Heating of Shapes Entering the Atmospheres of Venus and Mars at Super-orbital Speed," NASA TND-2064, 1963.

[24] James, C. S., "Experimental Study of Radiative Transport From Hot Gases Simulation in Composition the Atmospheres of Mars and Venus," [Reprint], 63-455, presented at AIAA Conference on Physics of Entry, August 1963.

[25] Dayman, B., et.a., "The Influence of Shape on Aerodynamic Damping of Oscillatory Motion during Mars Atmosphere Entry and Measurement of Pitch Damping at Large Oscillation Amplitudes," Tech. Rpt. No. 32-380, Jet Propulsion Lab., Pasadena, Calif.

[26] Kalaba, R., "On Non-linear Differential Equations, the Maximum Operation, and Monotone Convergence," J. of Math. and Mech., Vol. 8, No. 4, 1959.

[27] Isaacson, E., and Keller, H. B., "Analysis of Numerical Method," John Wiley and Sons, Inc., 1966.

[28] Schley, C. H., and Lie, L., "Optimal Control Computation by the Newton-Raphson Method and the Riccati Transformation," Preprints of Joint Automatic Control Conference, 1966, Univ. of Washington, Seatle, Washington.

[29] Pontryagin, L. S., et al., "The Mathematical Theory of Optimal Process," Interscience Publisher.

[30] Bryson, A. E., et al., "Optimal Programming Problems with Inequality Constraints: Necessary Conditions for Extremal Solutions," AIAA Journal, November 1963.

[31] Bellman, R., Glicksberg, I., and Gross, O., "On the 'Bang-Bang' Control Problem," Quarterly of Appl. Math., Vol. 14, No.1, April 1956.

[32] McGill, R., "Optimal Control, Inequality State Constraints, and the Generalized Newton-Raphson Algorithm," J. SIAM Control, Vol. 3, No. 2.

[33] Landau, L. D., and Lifshitz, E. M., "Fluid Mechanics," Russian Translation, Addison-Wesley Publ. Col., Inc., 1959.

[34] Parvin, R. H., "Inertial Navigation," Van Nostrand Co., Inc., October 1962.

[35] Pitman, G. R., "Inertial Guidance," John Wiley and Sons, Inc., January 1962.

[36] Schwartz, L., and Stear, E. B., "A Computational Comparison of Several Non-linear Filters," IEEE Trans. on AC, February 1968.

[37] Leondes, C. T., "Advances in Control Systems: Vol. 5," Academic Press, 1967.

[38] Doob, J. L., "Stochastic Processes," John Wiley and Sons, Inc., 1953.

[39] Stratonovich, R. L., "Conditional Markov Processes," Theory of Probability and Appl., Vol. 5, No. 2, 1960.

[40] Kushner, H. J., "On the Dynamical Equations of Conditional Probability Density Functions, with Applications to Optimal Stochastic Control Theory," J. of Math. Analysis and Appl. 8, 1964.

[41] Wonham, W. M., "Some Application of Stochastic Differential Equations to Optimal Non-linear Filtering," J. of SIAM Control, Ser. A2(3), 1964.

[42] Ito, K., "On Stochastic Differential Equations," Mem. Am. Soc. 4, 1951.

[43] Levin, J. J., "On the Matrix Riccati Equation," Proceeding of American Mathematical Socity, Vol. 10, 1959.

[44] Detchmendy, D. M., and Sridhar, R., "Sequential Estimation of States and Parameters in Noisy Nonlinear Dynamical Systems," Preprints, 6th JACC, Troy, New York, June 1965.

[45] Sridhar, R., "Fifth Quarterly Report to JPL," School of Elec. Eng., Purdue Univ., Lafayette, Indiana, April 1965.

[46] Kushner, H. J., "On the Differential Equations Satisfied by Conditional Probability Densities of Markov Process, with Applications," J. SIAM Control, Vol. 2, No. 1, 1962.

[47] Bellman, R. E., "Dynamic Programming," Princton Univ. Press, Princeton, New Jersey, 1957.

[48] Wonham, W. M., "Stochastic Problems in Optimal Control," RIAS Tech. Rpt. 63-14, May 1963.

[49] Gifford, F., "A Study of Martian Yellow Clouds that Display Movement," Monthly Weather Review, 92, October 1964.

[50] Uhlenbeck, G. E., and Ornstein, L. S., "On the Theory of the Brownian Motion," Physical Review, Vol. 36, No. 3.

[51] Ash, G. A., "Optimal Guidance of Low-Thrust Interplanetary Sapce Vehicle," Ph.D. Thesis, Calif. Inst. of Tech. Pasadena, Calif.

[52] Sahinkaya, Y., "Minimum Energy Control of Electric Propulsion Vehicles," Ph.D. Thesis, Calif. Inst. of Tech., Pasadena, Calif.

[53] Tung, F., "Linear Control Theory Applied to Interplanetary Guidance," IEEE Trans. AC, January 1964.

[54] Breakwell, J. V., and Tung, F., "Minimum Effort Control of Several Terminal Components," J. SIAM Control, Vol. 2, No. 3, 1965.

[55] Kushner, H. J., "Approximations to Nonlinear Filters," JACC 1967.

[56] Johnson, C. D., and Wonham, W. M., "On a Problem of Letov in Optimal Control," preprints 1964 JACC, 1964.

[57] Todd, J., "Survey of Numerical Analysis," McGraw-Hill Book Co., Inc., 1962.

[58] Merrian III, C. W., "Optimization Theory and Design of Feedback Control Systems," McGraw-Hill Book Co., 1964.

[59] Meditch, J. S., "On the Problem of Optimal Thrust Programming for a Lunar Soft Landing," IEEE Trans. on Automatic Control, Oct. 1964.

[60] Sanger, E., "Rakenten-Flugtechnik," R. Oldenboung (Berlin), 1933

[61] Jones, Bradley, "Elements of Practical Aerodynamics," John Wiley and Sons, Inc., 1939.

[62] Bellman, R. and Kalaba, R., "Selected Papers on Mathematical Trends in Control Theory," Dover Publications, Inc., New York.

[63] McGlinchey, L., "Voyager Pre-entry Capsule Control System," JPL Inter-office Memo 292-66-160, Aug. 1966.

[64] Jacobs, I. M., and Wozencraft, J. M., "Principles of Communication Engineering," John Wiley and Sons, Inc., 1965.

[65] Kushner, H. J., "Near Optimal Control in the Presence of Small Stochastic Perturbations," J. of Basic Engineering, Trans. of the ASME, March 1965.